Enhancement of Mobile Ad-hoc Network Models by Using Realistic Mobility and Access Control Mechanisms

Nasser M. A. Sabah

Submitted to the
Institute of Graduate Studies and Research
in partial fulfillment of the requirements for the Degree of

Doctor of Philosophy
in
Electrical and Electronic Engineering

Eastern Mediterranean University
May 2012
Gazimağusa, North Cyprus

Approval of the Institute of Graduate Studies and Research

Prof. Dr. Elvan Yılmaz
Director

I certify that this thesis satisfies the requirements as a thesis for the degree of Doctor of Philosophy in Electrical and Electronic Engineering

Assoc. Prof. Dr. Aykut Hocanın
Chair, Electrical and Electronic Engineering

We certify that we have read this thesis and that in our opinion it is fully adequate, in scope and quality as a thesis of the degree of Doctor of Philosophy in Electrical and Electronic Engineering

Assoc. Prof. Dr. Aykut Hocanın
Supervisor

Examining Committee

1. Prof. Dr. Mehmet Ufuk Çağlayan

2. Prof. Dr. Osman Kükrer

3. Assoc. Prof. Dr. Aykut Hocanın

4. Assoc. Prof. Dr. Hasan Demirel

5. Assoc. Prof. Dr. Muhammed Salamah

ABSTRACT

A mobile ad-hoc network (MANET) is a collection of wireless mobile nodes forming a temporary network without the need for base stations or any other preexisting network infrastructure. Ad-hoc networking received a great interest due to its low cost, high flexibility, fast network establishment, self-reconfiguration, high speed for data services, rapid deployment and support for mobility. However, in a wireless network without a fixed infrastructure and with nodes' mobility enabled, the topology keeps on changing. This causes frequent path changes and leads to an increase in network congestion and transmission delay.

Random waypoint (RWP) mobility model is widely used in ad-hoc network simulations. The model suffers from speed decay as simulation progresses, and may not reach the steady state in term of instantaneous average node speed. This usually leads to inaccurate results in protocol validation of MANETs modeling. The convergence of the average speed to its steady state value is delayed. Also, the probability distributions of speed vary over the simulation time, such that the node speed distribution at the initial state is different from the corresponding distribution at the end of the simulation. Gamma random waypoint (GRWP) mobility model has been proposed to overcome these problems. The nodes' speeds of GRWP are sampled from Gamma distribution. The analysis and simulation results indicate that the proposed GRWP mobility model outperforms the existing RWP mobility models.

In modeling wireless ad-hoc networks, the assumption of infinite population is usually

made. However, such models lead to deficiencies in the model, since they do not hold in real applications. Therefore, we model the wireless ad-hoc network as closed-form queueing network. In particular, the carrier sense multiple access with collision avoidance (CSMA/CA) based RTS/CTS handshake mechanism is modeled under finite population assumption. We take into account packet arrival time, network size, packet size, buffer size and backoff scheme. This is to ensure a realistic queueing model which describes the MAC protocol and nodes' behavior in the network environment more precisely. The collected results indicate that the finite population model gives an accurate and more realistic behavior of the RTS/CTS mechanism.

Keywords: Ad-hoc Networks, IEEE 802.11, MANETs, performance of MAC protocol, CSMA/CA, mobility models, RWP, Gamma distribution, finite population, blocking probability.

Öz

Tasarsız gezgin ağlar yer istasyonu veya daha önceden kurulmuş ağ yapısı gerektirmeyen ve gezgin düğümler tarafından geçici olarak oluşturulan ağlardır. Tasarsız ağlar, düşük maliyet, yüksek esneklik, hızlı kurulum, kendi kendine düzenleşim sağlama, yüksek hızda veri iletişim hizmeti sunma ve gezgin iletişime olanak tanıma özelliklerinden dolayı araştırmacılar tarafından ilgi toplamıştır. Herhangi bir telsiz ağda sabit bir altyapı bulunmadığından ve düğümlerin gezgin olmasından dolayı, ağ topolojisi sürekli değişmekte ve bunun sonucu olarak ağ tıkanıklığı ve iletim gecikmesi ortaya çıkmaktadır.

Rasgele yolgösterme (RWP) devingenlik modeli tasarsız ağların benzetiminde geniş olarak kullanılanmaktadır. Benzetim ilerledikçe, düğümlerin hızlarının azalması sorunu modelde gözlemlenmekte ve anlık hızların dağılımı kararlı duruma ulaşamamaktadır. Bu, doğru olmayan sonuçlara yol açmakta ve protokol doğrulanmasını güçleştirmektedir. Ayrıca, ortalama hız, kararlı hız değerine geç ulaşmakta ve düğüm hızların olasılık dağılımı benzetim süresince değişmektedir. Gamma yolgösterme devingenlik (GRWP) modeli bu sorunların giderilmesi için önerilmiştir. Benzetim sonuçları ve analitik türetimler GRWP modelinin mevcut modellere göre daha iyi başarıma sahip olduğunu göstermektedir.

Tasarsız gezgin ağların modellenmesinde genellikle sonsuz nüfus varsayımı kullanılmakta ama bu gerçek uygulamalarda eksikliklere yol açmaktadır. Bu nedenle, IEEE 802.11 RTS/CTS erişim protokolunda sonlu nüfus varsayımı kuyruk ağ modeli olarak kullanılmıştır. Paketlerin varış zamanı, ağın büyüklüğü ve yastık belleği göz

önüne alınmış ve MAC protokolundaki düğümlerin davranışları gerçekçi ve daha doğru olarak modellenmiştir.

Anahtar Kelimeler: Tasarsız ağlar, IEEE 802.11, MAC protokolu, devinim modeli, RWP, sonlu nüfus varsayımı.

ACKNOWLEDGMENTS

I am extremely grateful to my supervisor, Assoc. Prof. Dr. Aykut Hocanın, whose encouragement; guidance and unbounded support from the start to the final stage helped me to work hard. His commitment and motivation has immensely inspired me to achieve what I have always dreamt of. He has been not only a supervisor but a mentor throughout my PhD study at EMU. I would also like to thank Prof. Dr. Osman Kükrer for his valuable assistance and help during my study and research.

I would like to thank my thesis monitoring committee members: Prof. Dr. Derviş Z. Deniz, Assoc. Prof. Dr. Hüseyin Bilgekul and Asst. Prof. Dr. Hassan Abou Rajab. I would like to express my gratitude to all professors and staff at Electrical and Electronic Engineering department for giving me moral support during my study and research at EMU. I would also like to thank my colleagues and friends, Mohammad Salman and Alaa Elyan for their friendship and companionship during my study at EMU. Special thanks are given also to my officemates at Palestine Technical College for their support.

I am greatly indebted to my parents whom I know are happy for what I have achieved. My deepest gratitude goes to my wife and kids for giving me strength and inspiration, unconditional love and encouragement during my research. Personal thanks to my family who have always believed in all my endeavors. Last but not the least; I would like to thank Almighty Allah for giving me the opportunity to fulfill my dream and to work with people who truly made a difference in my outlook in life.

DEDICATION

For the soul of my parents

For the soul of our symbol Yasser Arafat

TABLE OF CONTENTS

LIST OF FIGURES

LIST OF TABLES

LIST OF SYMBOLS AND ABBREVIATIONS

A	Simulated area
$F_T(t)$	CDF traveling time
G	Offered load
N	Total number of nodes
N_{nbr}	Nodes' density
$P[0]$	Probability of zero transmission
P_c	Probability of collision transmission
P_s	Probability of successful transmission
P_{tr}	Probability of transmission
R	Transmission range
S	Throughput
T	Packet transmission time period
T_c	Collision transmission time period
T_s	Successful transmission time period
T_{busy}	Busy time period
T_{idle}	Idle time period
V_{ss}	Steady state speed
V_{max}	Maximum traveling speed
V_{min}	Minimum traveling speed
Y	Period of second packet occurrence
d	Traveling distance

$f_T(t)$	PDF traveling time
$f_V(v)$	PDF traveling speed
$f_{V_{ss}}(v)$	PDF steady state speed
m	Backoff stage
p	Probability of a node transmission
t	Traveling time
t_p	Pausing time
v	Traveling speed
$\bar{v}$	Instantaneous average node speed
α	Shape parameter of Gamma distribution
β	Scale parameter of Gamma distribution
γ	End-to-end propagation delay ratio
δ	Slot time
δ_{idle}	Duration of idle slot time
λ	Packet arrival rate
μ	Mean
σ	Standard deviation
τ	One way propagation delay

ACK	Acknowledgement
BBR	Basic Bit Rate
BCC	Blocked Customers Cleared
BCD	Blocked Customers Delayed

BEB	Binary Exponential Backoff
BERs	Bit Error Rates
CBR	Constant Bit Rate
CDF	Cumulative Distribution Function
CDMA	Code Division Multiple Access
CSMA	Carrier Sense Multiple Access
CSMA/CA	CSMA with Collision Avoidance
CSMA/CD	CSMA with Collision Detection
CTS	Clear to Send
CW	Contention Window
DCF	Distributed Coordination Function
DFWMAC	Distributed Foundation Wireless MAC
DIFS	Distributed Inter-frame Space
DMAC	Distributed and Mobility Adaptive Clustering
DSSS	Direct Sequence Spread Spectrum
FAMA	Floor Acquisition Multiple Access
FDMA	Frequency Division Multiple Access
FHSS	Frequency-Hopping Spread Spectrum
GRWP	Gamma RWP
IFS	Inter-frame Spaces
IID	Independent and Identical Distributed
IRP	Independent Random Point
LBT	Listen-Before-Talk

MAC	Medium Access Control
MACA	Multiple Access with Collision Avoidance
MACAW	Multiple Access with Collision Avoidance for Wireless
MANETs	Mobile Ad-Hoc Networks
NAV	Network Allocation Vector
OFDM	Orthogonal Frequency Division Multiplexing
PCF	Point Coordination Function
PDF	Probability Density Function
PDR	Packet Delivery Ratio
ROHC	Robust Header Compression
RTS	Ready to Send
RWP	Random Waypoint
S-ALOHA	Slotted Aloha
SIFS	Short Inter-frame Space
SNR	Signal to Noise Ratio
TDMA	Time Division Multiple Access
UWB	Ultra Wide Band
VANETs	Vehicular Ad-Hoc Networks
WLANs	Wireless Local Area Networks

Chapter 1

INTRODUCTION

1.1. Background

A wireless ad-hoc network is a collection of wireless mobile nodes that self-configure to form a network without the aid of any established infrastructure. Nodes are responsible for network control and management. A node may communicate with any other node by establishing peer-to-peer connections. Depending on the distance between two nodes, their connection may either be a direct connection that is consisted of a single hop or a multi-hop connection, where data is relayed to the destination through intermediate nodes.

Wireless local area networks (WLANs) are types of ad-hoc networks that employ a common medium for communications, where all nodes access a share medium. If more than two nodes transmit frames at the same time, a collision occurs at the receiving nodes. All frames involved in the collision are lost and the medium is wasted during this collision interval. As the active transmitting nodes increase, the probability of collisions increase and much of the shared medium bandwidth will be wasted due to collision. When a node experiences a collision, it chooses independent random backoff delay time before retransmitting the frame, it is possible that a node will choose a delay that is sufficiently less than the delays of the other colliding nodes, and will be able to

retransmit its frame faster than other collided nodes and without a collision. Therefore, a multiple access protocol is needed to regulate the function sharing common resource fairly and effectively among the distributed nodes, minimize collisions between nodes, provide better connectivity environment and efficient resource utilization.

1.2. Contributions

In this thesis, two main contributions are presented: Most of the existing research on mobility models focused on nodes' distribution and disregarded the choice for speed distribution even though it is a significant and challenging problem. A modified RWP mobility model is proposed with a more precise distribution of the nodes' speed. The speeds of nodes are sampled from Gamma distribution because of its capability of modeling nodes' speed variations effectively. This model has been proposed to overcome some of the difficulties experienced with the existing RWP mobility models, such as speed decay and the variation of probability distributions of speed over the simulation time. The proposed mobility model captures the movement behaviors of ad-hoc nodes in real environments effectively and also achieves higher steady state speed which is close to the pre-assumed average speed. The novelty of this work resides in the derivation of the steady state speed of the proposed GRWP mobility model. Additionally, we study the effect of mobility patterns on the IEEE 802.11 performance in terms of throughput, delay and retransmission rate.

The second main contribution is the proposed finite queueing model of the IEEE 802.11 ad-hoc network. In particular, we model the CSMA/CA based RTS/CTS handshake mechanism as a closed-form *M/M/1/K/N* queueing network. This is to ensure a realistic queueing model which describes the IEEE 802.11 MAC protocol and nodes'

behavior in the network environment more precisely. The IEEE 802.11 wireless networks of the RTS/CTS access mechanism is modeled under a finite population assumption. Matlab simulation environment is used to validate the queueing model. The simulation results indicate that finite population queueing model gives an accurate description of the IEEE 802.11 RTS/CTS access mechanism and realistic behavior of nodes in the network.

1.3. Thesis Outline

The contents of the thesis are organized as follows: Following the general introduction and our contributions in Chapter 1, Chapter 2 provides a detailed study of the IEEE 802.11 Protocols (i.e., GSMA and GSMA/CA) and random mobility models.

Chapter 3 introduces the proposed GRWP mobility model. Related work in nodes' speed distribution and stochastic properties of RWP mobility model that are useful in the derivation of the nodes' speed distribution are included. The analytic expressions for the speed distribution are derived and illustrated for several scenarios. Moreover, the detailed analysis and derivations of the proposed mobility model are presented. Chapter 4 presents the mobility effect on the performance of the IEEE 802.11 DCF MAC protocol. The protocol is tested under various speed distribution patterns of RWP mobility model.

A queueing model of wireless ad-hoc networks is presented in Chapter 5. The IEEE 802.11 wireless network of the RTS/CTS access mechanism is modeled under finite population assumption. This queueing model describes the MAC protocol and nodes' behavior in the network environment more precisely. Chapter 6 presents the simulation

results of the proposed schemes through simulations. Simulation results are presented to validate the performance of the proposed GRWP mobility model, effect of mobility on the CSMA/CA based RTS/CTS handshake mechanism (throughput, system delay and network connectivity) and the finite queueing model of the RTS/CTS access mechanism. Finally, Chapter 7 summarizes the main findings of this work and concludes the thesis.

Chapter 2

PERFORMANCE ANALYSIS OF IEEE 802.11 ARCHITECTURE AND PROTOCOLS

2.1. Introduction

Wireless networks are generally classified into two working modes, centralized (infrastructure) mode and ad-hoc (distributed) network modes. In centralized wireless network mode, a central base station acts as an interface between the wireless and infrastructure wireline networks. Also, the base station is responsible to assign time slots for channel protocols among all nodes to achieve efficient channel utilization in the wireless network. In the wireless ad-hoc network mode, there is no such central administration that controls and assists the nodes. However, these wireless nodes still operate independently and are expected to achieve efficient channel utilization in the wireless network. In this thesis, our focus will be on the distributed ad-hoc network mode. Figure 2.1 shows an example of an ad-hoc network mode.

Ad-hoc networking received a great interest due to its low cost, high flexibility, fast network establishment, self-reconfiguration, high speed for data services, rapid deployment and support for mobility. Ad-hoc networks can be used in situations where the infrastructure is not presented, infrastructure has been damaged or it is difficult to install any fixed communication infrastructures. It has been widely used in military

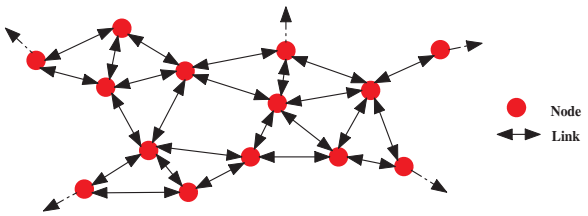

Figure 2.1. Example of wireless ad-hoc network mode.

and battlefield scenarios, disaster areas, remote areas, short term ad-hoc conferences and home networking between various appliances.

Mobile ad-hoc networks (MANETs) are composed of wireless mobile nodes that form a temporary multi-hop wireless networks without the need of base stations or any other preexisting network infrastructure. Mobile nodes communicate with each other in a peer-to-peer fashion by using wireless multi-hop communication. However, in a wireless network without a fixed infrastructure and with nodes' mobility enabled, the topology keeps on changing. This causes frequent path changes and leads to increase the network congestion and transmission delay over the network.

2.2. IEEE 802.11 Architecture

Wireless ad-hoc networks may be used when a fixed communication infrastructure for wired or wireless networks does not exist or has been destroyed. The goal of such wireless network is to allow a group of communicating nodes to setup and maintain connections among themselves without the support of a base station. The 802.11 IEEE standard [1] is well established as the MAC protocol for wireless local area networks (WLANs) and has been extensively studied in ad-hoc settings, either through simula-

tions or through real hardware deployments [2]. The 802.11 standard consists of three main parts, the physical layer specification, the MAC specification and the power saving functionality that operates on both physical and MAC layer. Figure 2.2 shows the IEEE 802.11 elements, access scheme and the offered services.

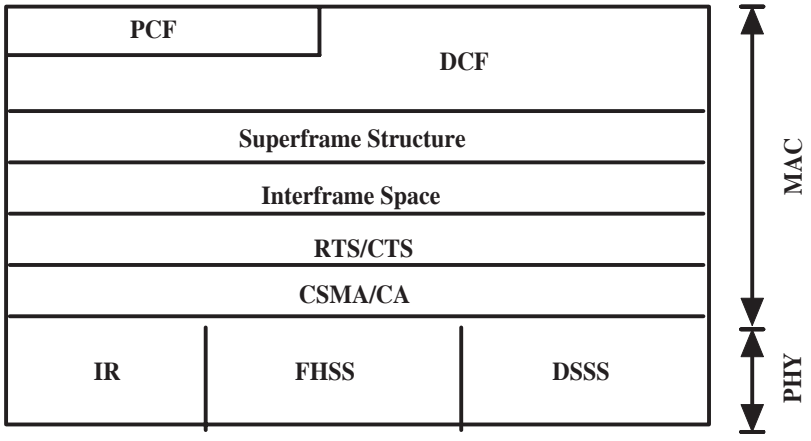

Figure 2.2. IEEE 802.11 system architecture [1].

2.2.1. The Physical Layer

The physical layer at the transmitting node is responsible for converting data bits to electrical or electromagnetic waves and vice versa. At the transmitting side, a data stream is first partitioned into blocks which are often referred to as messages, packets or frames. The IEEE 802.11 draft standard specifies three physical layers, each for a distinct transmission technology. The first specification employs baseband infrared transmission (IR) and the other two specifications employ radio direct sequence spread spectrum (DSSS) and frequency-hopping spread spectrum (FHSS) technology. Plain 802.11 provides bit rates of 1 or 2 Mbps transmission in the 2.4 GHz band using either FHSS or DSSS. 802.11a is an extension to 802.11, provides bit rates of 6, 9, 12, 18,

24, 36, 48 and 54 Mbps in the 5GHz band, using an orthogonal frequency division multiplexing (OFDM) encoding scheme. 802.11b provides bit rates of 1, 2, 5.5 and 11 Mbps transmission in the 2.4 GHz band using DSSS. 802.11g provides nominal data rates up to 54 Mbps in the 2.4 GHz using DSSS.

2.2.2. Medium Access Control

MAC sub-layer is located in the data link layer, where its main objective is to access and control the shared limited bandwidth medium efficiently and fairly among all nodes in the network. More specifically, the key objective of most MAC protocols is to achieve high network throughput. However, higher network throughput and better performance can be achieved by reducing the data retransmission. Solving the hidden terminal problem will decrease the collision rate of transmission while increasing the medium utilization [3].

MAC protocols are extensively studied in traditional wireless networks and can be categorized into two approaches, collision-free protocols and contention protocols. Pre-allocated transmissions are collision free protocols. It is widely used in modern cellular communication systems due to its collision free structure, such as in time division multiple access (TDMA), frequency division multiple access (FDMA) and code division multiple access (CDMA). The principle idea is to avoid interference by scheduling nodes into different sub-channels that are divided either by time, frequency or orthogonal codes respectively. While contention based protocol is an advanced wireless protocol and is normally used in multi-hop wireless networks. Carrier sense multiple access (CSMA) is example of contention-based MAC protocols, where nodes

share the same medium.

MAC layer offers two type of service: contention service and contention-free service [4]. Contention service with stochastic bandwidth sharing is used by the distributed coordination function (DCF); it is based on carrier sense multiple access with collision avoidance (CSMA/CA) scheme with rotating backoff for the distributed medium sharing, where DCF is available in the ad-hoc mode. Contention-free service with support for limited delay is used via the point coordination function (PCF); it is based on the polling based reservation scheme. Both coordination modes coexist simultaneously within a super-frame structure in the infrastructure mode.

In order to separate different type of packets and different levels of access priority, inter-frame spaces (IFS) of varying length are implemented as defined in the 802.11 standard [4]. It defines the minimum time that a node has to wait before start transmitting a certain type of packet. Short inter-frame space (SIFS) is the inter-frame space for small control frames used for acknowledgements and collision avoidance. Distributed inter-frame space (DIFS) is a larger inter-frame space for data frames. The use of IFS allows the most important frames to be sent without any additional delay and without having to compete for access with lower priority frames. It facilitates the prioritized access to the medium.

2.3. Carrier Sense Multiple Access

Carrier sense multiple access (CSMA) protocols use the listen-before-talk (LBT) methodology based on sensing activity to achieve high throughput efficiency. It is currently the main mechanism that implement the distributed medium access [5]. In addition,

it is a probabilistic MAC protocol in which a transmitter node senses the medium before attempting any transmission. If the medium is sensed busy, the node waits for the transmission in progress to finish before initiating its own transmission. Multiple nodes send and receive packets on the shared medium, where the transmission of one node is generally received by all other neighboring nodes.

In a large geographical area with nodes spread a part, the communication environment may change from a single-hop to a multi-hop communication. CSMA based MAC protocol may works well in a single-hop environment, but may suffer performance degradation in a multi-hop environment due to the hidden node problem [6, 7]. Another problem of CSMA in a multi-hop wireless network is the exposed terminal problem, the existence of exposed nodes result in a reduced medium utilization. However, solving the hidden and exposed node problem in the multi-hop environment can decrease the probability of collision in transmission, resulting in an increased of network throughput. The CSMA is classified into two types: Persistent and non-persistent CSMA.

2.3.1. Persistent CSMA

There are two versions of persistent CSMA [8]: P-persistent CSMA and 1-persistent CSMA.

- P-persistent CSMA

  In which when a node is ready to send data; the protocol continuously senses the transmission medium to maximize the network throughput. If the medium is idle, then the node transmits a frame with a probability p and defers for one slot

time with a probability $1 - p$. If the medium is busy, the node defers and waits the medium to become idle, then transmits its data with the same probability p. In case of collision, the node waits for a random time as shown in figure 2.3. The network throughput increases as long as p decreases from 1 to 0.01. However, if p is too small, the delay will be very large, which leads to lower spatial reuse [9].

- 1-persistent CSMA

  It is a special version of p-persistent CSMA. The procedure of 1-persistent CSMA is the same as in p-persistent CSMA, except that if the medium is busy, node waits until the medium becomes idle and transmits data with a transmission probability $p = 1$. When a node is ready to send data, and if the medium is idle, then the node transmits its data immediately. If the medium is busy, the node continuously senses the medium until it becomes idle and transmits its data immediately with a probability of 1. In case of collision, the node waits for a random time and starts over again [10].

2.3.2. Non-persistent CSMA

Non-persistent CSMA eliminates most of the collisions in the persistent CSMA. In non-persistent CSMA, when a node has data to transmit, it senses if the medium is idle. If so, it transmits its data immediately. However, if the medium is busy, the node defers for a random backoff time and senses the medium again after the expiration of the backoff timer. In case of a collision, the node chooses a random backoff time and retransmits its data when the random backoff timer is expired as shown in the flow

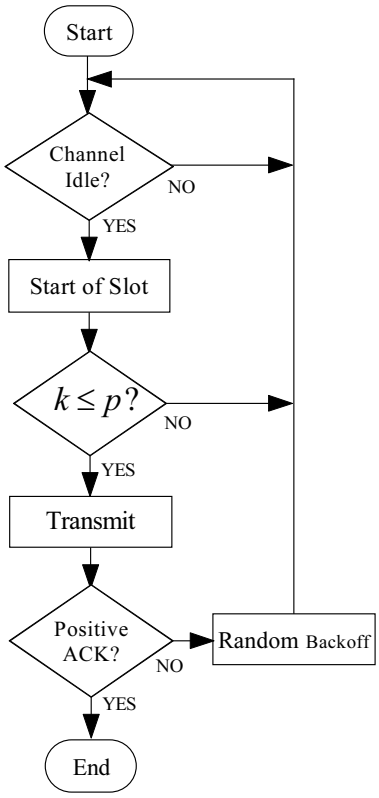

Figure 2.3. Slotted p-persistent CSMA flow chart.

chart of figure 2.4.

In evaluating the performance of non-persistent CSMA; assuming fixed packet length, constant packet transmission time in unit of time (T seconds) and mean arrival rate of packet λ according to poisson process (packets/sec). Packets (new and retransmitted) arrive according to poisson process. Also, the probability of k transmission attempts in a given frame time for both new and retransmitted packets is also a poisson distribution.

As shown in figure 2.5, the node starts transmitting at time t for a period of packet transmission time (T seconds). The destination node will receive the packet after propagation delay of τ seconds. Therefore, this transmission causes the medium to be busy

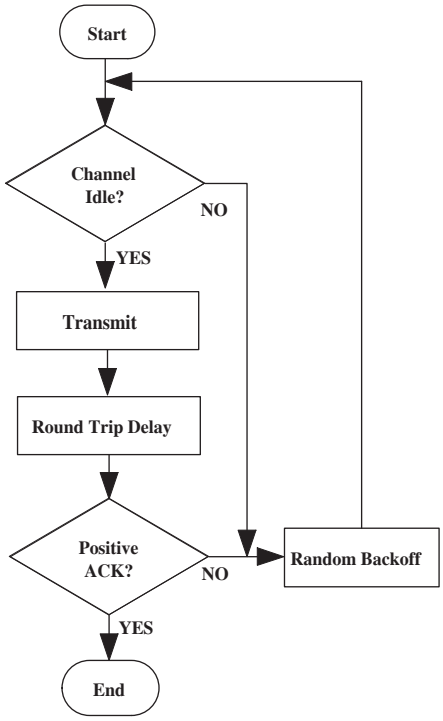

Figure 2.4. Non-persistent CSMA flow chart.

for a period of $(T + \tau)$ seconds. If any node attempts to access the medium after the vulnerable period τ, that node will find the medium busy and chooses a random backoff time. However, if any node attempt to access the medium during the period $(t, t + \tau)$, this node would sense the medium idle and start transmitting its packet, this will cause a collision. The initial period of the first t seconds of transmission is called the vulnerable period, this is because the transmission is vulnerable to interference within this period only. The packet is successfully transmitted if no nodes transmit packet during this vulnerable period.

In analyzing the non-persistent CSMA, throughput S is defined as the fraction of time used for successful transmissions of packets in the medium. The normalized through-

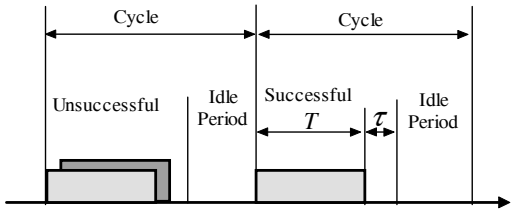

(a) Busy and idle periods

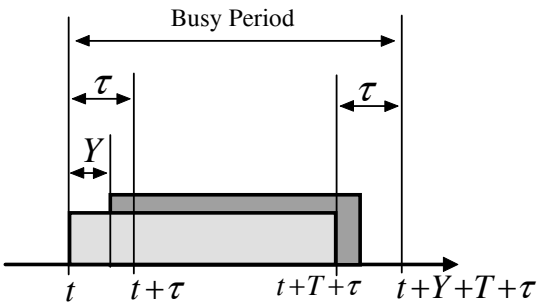

(b) Unsuccessful transmission period

Figure 2.5. Non-persistent CSMA [11].

put S is given by [12]:

$$\begin{aligned} S &= \frac{E\left[\text{payload transmitted in a slot time}\right]}{E\left[\text{length of a slot time}\right]}, \\ &= \frac{E[T_D]}{E[T_{busy}] + E[T_{idle}]}, \end{aligned} \tag{2.1}$$

where $E[T_D]$ is the expected duration of a successful transmission of a data packet, $E[T_{busy}]$ is the expected duration of a busy time period and $E[T_{idle}]$ is the expected duration of an idle time period.

The expected duration of the idle time period $E[T_{idle}]$ is defined as the ratio of packet transmission time (T seconds) and the offered load $G = \lambda T$, is given by

$$E[T_{idle}] = \frac{T}{G}. \tag{2.2}$$

The average duration of a busy time period $E[T_{busy}] = E[T + \tau + Y]$, where Y is the period of second packet occurrence (see figure 2.5(b)). The CDF of Y is given as follows

$$\begin{aligned} F_Y(y) &= Pr[\text{zero arrival in the interval}(\tau - y)] \\ &= e^{-\lambda(\tau - y)}. \end{aligned} \tag{2.3}$$

Taking the derivative of (2.3) with respect to the period occurrence of Y, the PDF of Y is given as follows

$$f_Y(y) = \lambda\, e^{\lambda(y-\tau)}. \tag{2.4}$$

The expected value of Y (see APPENDIX 1) is given as follows

$$\begin{aligned} E[Y] &= \int_0^\tau y\, f_Y(y)\, dy \\ &= \int_0^\tau y\lambda\, e^{\lambda(y-\tau)}\, dy \\ &= \tau - \frac{1 - e^{-\lambda\tau}}{\lambda}. \end{aligned} \tag{2.5}$$

Substituting (2.5) in the given average duration of a busy time period, $E[T_{busy}]$ becomes

$$E[T_{busy}] = T + 2\tau - \frac{1 - e^{-\lambda\tau}}{\lambda}. \tag{2.6}$$

The average time for a successful transmission of a data packet is defined as the product of the probability of successful transmission and the packet transmission time, $E[T_D]$ is given as follows

$$E[T_D] = P_s\, T, \tag{2.7}$$

where P_s is the probability of a successful transmission and is defined as the probability that no packet is scheduled during the vulnerable period, $P_s = P[0] = e^{-\gamma G}$. $E[T_D]$ is given as follows

$$E[T_D] = T\, e^{-\gamma G}, \tag{2.8}$$

where $\gamma = \frac{\tau}{T}$ is the end-to-end propagation delay; which is the normalized propagation ratio. τ is the maximum one way propagation delay time.

Substituting the values of $E[T_D]$, $E[T_{busy}]$ and $E[T_{idle}]$ in (2.1), and after further simplification of terms, the throughput becomes

$$\begin{aligned} S &= \frac{T\, e^{-\gamma G}}{T + 2\tau - \frac{1-e^{-\lambda\tau}}{\lambda} + \frac{T}{G}} \\ &= \frac{G e^{-\gamma G}}{G\,(1 + 2\gamma) + e^{-\gamma G}}. \end{aligned} \tag{2.9}$$

Figure 2.6 shows the throughput of non-persistent CSMA for various values of γ. The transmission is vulnerable to interference within the vulnerable period $(t, t + \tau)$, the throughput can reach $\%100$ when γ becomes zero. During the vulnerable period, nodes

would sense the medium as idle and they start transmitting their data packets, causing a collision. As the propagation delay increases (increasing the vulnerable period), the probability of attempting transmission during this period is increased, which decrease the throughput since more packets collide.

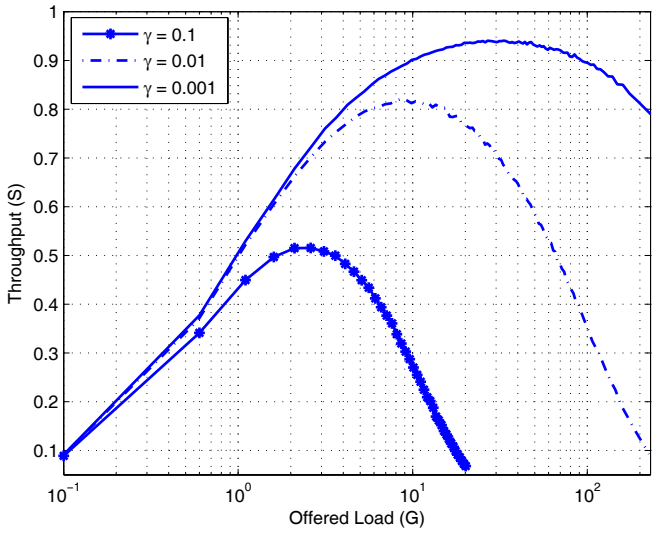

Figure 2.6. Throughput of non-persistent CSMA.

Figure 2.7 shows the average system delay of the non-persistent CSMA for various values of γ. When $\gamma = 0.001$ (minimal propagation delay), the average system delay is very small. This is because the attempted numbers of retransmission packets are minimal due to less collision of packets. As the value of propagation delay increases, more packet collisions occur and result in increased of retransmission attempts. This will cause the collided packets to collide again during retransmissions, thus the average system delay increases exponentially due to the poisson distributed arrival of packets.

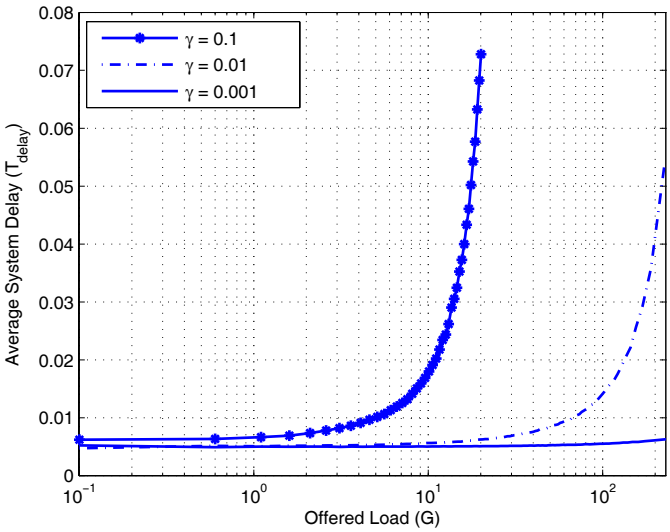

Figure 2.7. Average system delay of non-persistent CSMA [13].

2.3.3. Slotted Non-persistent CSMA

Slotted non-persistent CSMA is similar to CSMA protocols except for a slotted time axis, where time slot size equals the maximum propagation delay τ [13]. Nodes can transmit at the beginning of a time slot only. If a node has a data and is ready to transmit, it checks if the physical medium is busy. If so, the node waits for a random backoff time, then senses the physical medium again. If the physical medium is idle, then the node transmits its data at the next time slot. In case of a collision, the node waits for a random backoff time and attempts to transmit again as shown in the flow chart of figure 2.8.

Probability of successful transmission is defined as the ratio of the probability of exactly one transmission attempt and the probability of at least one transmission attempt

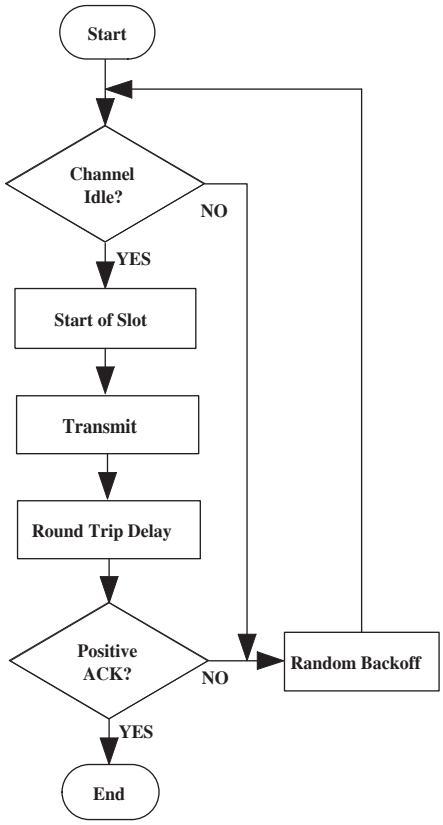

Figure 2.8. Slotted non-persistent CSMA flow chart.

in a given time slot. P_s is obtained as follows

$$\begin{aligned} P_s &= \frac{P(k=1)}{P(k\geq 1)} = \frac{P[1]}{1-P[0]} \\ &= \frac{\gamma\, G\, e^{-\gamma G}}{1-e^{-\gamma G}}. \end{aligned} \tag{2.10}$$

Substituting (2.10) in (2.7), the average time for successful transmission of data packets $E[T_D]$ becomes

$$E[T_D] = \frac{T\,\gamma\, G\, e^{-\gamma G}}{1-e^{-\gamma G}}. \tag{2.11}$$

The average duration of a busy time period is defined as the sum of packet transmission time and end-to-end propagation delay, $E[T_{busy}]$ is given as follows

$$E[T_{busy}] = T + \tau. \tag{2.12}$$

The expected duration of an idle time period $E[T_{idle}]$ is proportional to the probability that no node transmits during the last slot with width γ in the idle period, $E[T_{idle}]$ is given by [13]:

$$E[T_{idle}] = \frac{\tau\ e^{-\gamma G}}{1 - e^{-\gamma G}}. \tag{2.13}$$

Substituting the values of $E[T_D]$, $E[T_{busy}]$ and $E[T_{idle}]$ in (2.1), and after further simplification of terms, the throughput becomes

$$S = \frac{G\ e^{-\gamma G}}{\gamma + (1 - e^{-\gamma G})}. \tag{2.14}$$

As shown in figure 2.9, the slotted non-persistent CSMA outperforms the non-persistent CSMA at all values of γ. The maximum achieved throughput is about 0.96 at $\gamma = 0.001$. As γ increases, the vulnerable period increases and the throughput decreases because more packets are collided. Also, as the value of G increases, the probability of attempting transmission increases and the number of collision frames increased. As a result, the throughput decreases because of more packets are collided.

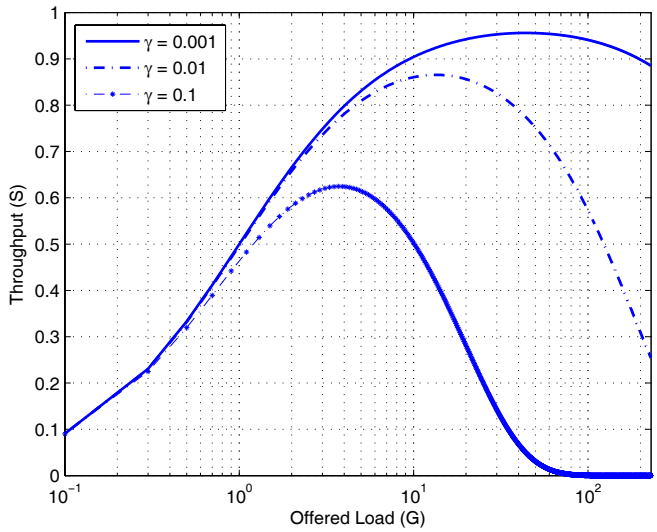

Figure 2.9. Throughput of slotted non-persistent CSMA.

2.4. CSMA with Collision Avoidance

CSMA with collision avoidance (CSMA/CA) is a modification of pure CSMA. Collision avoidance is used to improve the CSMA performance; where it forces the CSMA to be less greedy and allows only a single nodes' transmission on the medium at a time. If a node intends to initiate a transmission and senses the medium as busy, then the transmission is deferred for a random interval. Thus, collision avoidance reduces the probability of packets collisions by using a random binary exponential backoff (BEB) time.

The 802.11 based CSMA/CA is commonly used in WLANs. Collision detection is one of the problems facing WLANs, where it is difficult for a node to listen to its transmission while sending. Other problems are the hidden and the exposed terminal problem as illustrated in figure 2.11. The hidden terminal problem requires special

attention when designing the MAC for the wireless environment. DCF defines two access mechanisms for packet transmission: The basic access mechanism (2-ways handshaking) and RTS/CTS (Request to Send/Clear to Send) virtual carrier sensing mechanism (4-ways handshaking).

2.4.1. CSMA/CA Two Ways Handshake

The basic access mechanism (2-ways handshaking) is shown in figure 2.10. It should be noted that this scheme suffers from the hidden terminal problem.

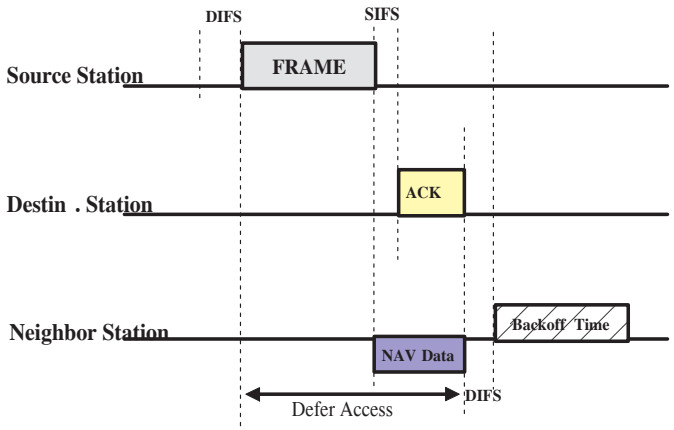

Figure 2.10. Basic access mechanism [14].

Hidden terminals [15] are nodes that are in range of the destination node but not in range of the source node. Collisions occur when hidden terminal nodes unable to sense the source's transmission, attempt to transmit simultaneously, causing a collision at the destination node. Figure 2.11(a) illustrates the hidden terminal problem scenario, where node B is in the transmission range of both nodes A and C, but node A and C cannot hear each other. Let assume that node A is transmitting to node B. According to

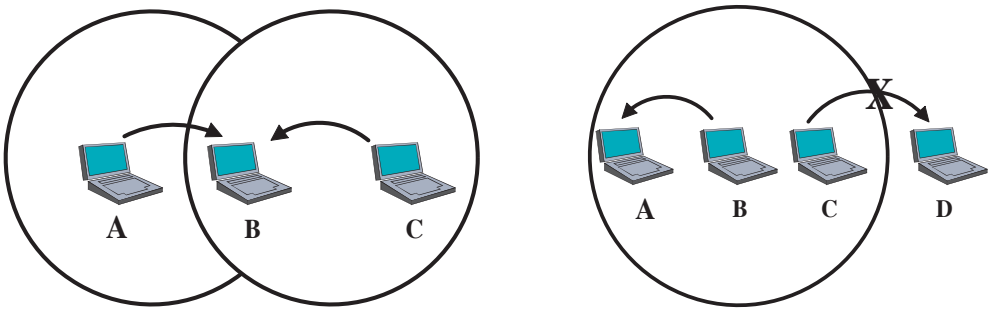

(a) (b)

Figure 2.11. (a) Hidden terminal problem. (b) Exposed terminal problem.

the DFC protocol, if node C has a frame to transmit to node B, also node C does sense that node B is participating in a transmission. Node C may initiate a transmission but this transmission will result in a collision at the destination node B.

Figure 2.11(b) illustrates the exposed terminal problem scenario [17]: Let's assume that both node A and C can hear transmission from node B. Let node B is transmitting to node A. According to the DFC protocol, if node C has a frame to send to node D, then it senses that the medium is busy because of the ongoing transmission of B. Therefore, it refrains from initiating its transmission to D, despite this transmission will not cause a collision at node A. Thus the exposed terminal problem may leads to a throughput reduction.

Considering a cell in a network, and assume that all nodes are in line of sight with each other and no hidden nodes. Packet generation can be modeled as Bernoulli trials, hence the geometric distribution of the idle time slot is $(1-P[0])P[0]^{i-1}$. The expected

duration of an idle time slot is given by

$$E[T_{idle}] = \delta \sum_{i=1}^{\infty} i \left(1 - P[0]\right) P[0]^{i-1} = \frac{\delta}{1 - P[0]}, \tag{2.15}$$

where $P[0]$ is the probability of no packet initiated in the same time slot, $1 - P[0]$ is the probability that at least one packet initiate a transmission in the same time slot. i is the number of consecutive idle slots and δ is the duration of time slot.

Busy time slots N_{busy}, is defined as the average number of slots for which at least one packet is initiated during these slots, is given by

$$N_{busy} = \sum_{i=1}^{\infty} iP[0] \left(1 - P[0]\right)^{i-1} = \frac{1}{P[0]}. \tag{2.16}$$

Probability of successful transmission is given as follows

$$\begin{aligned} P_s &= \frac{P(k=1)}{P(k \geq 1)} \\ &= \frac{P[1]}{1 - P[0]}. \end{aligned} \tag{2.17}$$

A successfully transmission occurs at $(N_{busy}P_s)$ slots and a collision transmission occurs at $(N_{busy}(1 - P_s))$ slots. Therefore the expected duration of a busy period time slots is defined as the product of the slot period and the total number of slots in which

a successful and a collision transmission occur, is given by

$$\begin{aligned} E[T_{busy}] &= T_s\, N_{busy}\, P_s + T_c\, N_{busy}(1 - P_s) \\ &= \frac{T_c + P_s(T_s - T_c)}{P[0]}. \end{aligned} \tag{2.18}$$

where the successful and collision transmissions of IEEE 802.11 basic access mechanism are given by:

$$\begin{aligned} T_s &= T_D + T_{ACK} + SIFS + DIFS + 2\tau \\ T_c &= T_D + DIFS + \tau, \end{aligned} \tag{2.19}$$

The average time of transmitting a data packet is given by

$$\begin{aligned} E[T_D] &= T_D\, N_{busy}\, P_s \\ &= \frac{T_D\, P[1]}{P[0]\,(1 - P[0])}. \end{aligned} \tag{2.20}$$

Substituting the values of $E[T_D]$, $E[T_{Busy}]$ and $E[T_{idle}]$ in (2.1). Normalized throughput S is given as follows

$$S = \frac{T_D\, P_s}{T_c + P_s(T_s + T_c) + \delta P[0](1 - P[0])}. \tag{2.21}$$

2.4.2. CSMA/CA Four Ways Handshake

The IEEE 802.11 group realized the necessity to address the hidden terminal problem and integrated the RTS/CTS virtual carrier sensing mechanism (4-ways handshaking). The RTS/CTS protocol is a common MAC protocol for WLANs such multiple access with collision avoidance (MACA) [16], MACA for wireless (MACAW) [17], floor acquisition multiple access (FAMA) [18] and IEEE 802.11 [19]. The main aims of the protocol are to coordinate for the data packet transfer between source and destination node. Also, to broadcast the duration of packet transfer to nodes those are in range of the source and destination nodes. The RTS/CTS increases bandwidth efficiency by reducing the collision probability, although it utilizes more bandwidth by transmitting two additional control packets per data packet transmission. This partially solves the hidden terminal problem in the basic access. However, the virtual carrier sensing mechanism requires the destination nodes to decode the MAC header of the RTS and CTS control packets correctly. Also, the performance of the RTS/CTS handshake mechanism degrades rapidly as the number of nodes in the network increased moderately, this is due to the much reduced spatial reuse [20]. The RTS/CTS is typically used in MANETs, this is because it increases the bandwidth efficiency by reducing the collision probability and expends more bandwidth by transmitting two additional control packets per data packet transmission. The authors in [21], evaluated the performance of IEEE 802.11 DCF in WLAN, they show a better performance of RTS/CTS handshake mechanism over the basic access mechanism in a high traffic network.

The RTS/CTS protocol is used when the length of data packets are long, this is to avoid the possible long collision period of data packets. As shown in figure 2.12, prior to data

packet transmission, the source node does not send data packet immediately, but rather transmits an RTS control packet containing the frame duration information. If the destination node is in range with the source node and receives the RTS correctly, it replies with a CTS control packet after waiting for a period of time equal to the SIFS time, this CTS also informs the destinations' neighborhood about the incoming packet reception. The source node responds to the CTS by transmitting the data packet after SIFS time. However, if CTS is not received by the source node within a specified timeout period, the source node assumes that the RTS had a collision at the destination node; then the source node chooses a random backoff time and retransmits the RTS after the backoff time period reaches zero. Other nodes that overhear either the RTS or CTS must defer their own transmissions for the duration of the data packet transmission. After the data packet is being received, the destination node waits for a SIFS time and then sends an ACK control packet to inform the source of data packet reception. The CSMA/CA scheme will be explained in details in Chapter 4 based in the assumption of Bianchi model [14].

A node may overhear various reservation requests from other nodes. Based on the received reservation requests, a data structure called network allocation vector (NAV) is used to maintain the aggregate duration of time in the current transmission and to schedule transmissions to avoid collision. The NAV of all other nodes is set to the frame duration information in RTS, CTS, Data and ACK headers; these nodes has to wait out this NAV duration before contending for medium access [22]. Also the NAVs are updated without any further communication.

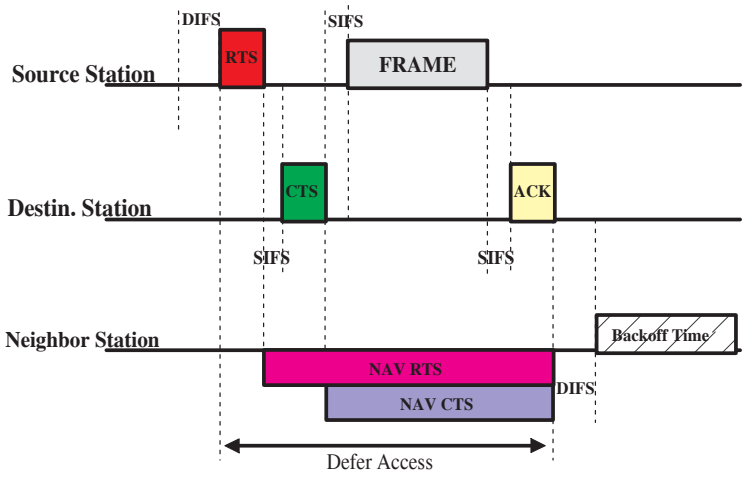

Figure 2.12. CSMA/CA scheme with the RTS/CTS handshake mechanism [14].

2.5. Random Mobility Models

Random mobility models are synthetic entity models that describe the mobility pattern of nodes' behaviors without the use of traces, where the speed or direction of mobile nodes remains constant for one movement period. The current speed and direction of a mobile node is independent of its past speed and direction, in which a mobile node moves freely without constraint on its speed, time period and destination [23]. A survey studies of synthetic mobility models are presented in [24, 25].

Most of the existing simulation and analytical studies of MANETs assume that mobile nodes are uniformly distributed in the network. In theoretical analysis, the assumption of uniform node distribution can provide appropriate solution for the derivation and evaluation of network throughput, this is regardless of the undesired influence of non-uniform node distribution induced by mobility models [26, 27]. However, the existing random mobility models can mislead the performance evaluation of MANETs [28, 29].

Therefore, an efficient and accurate mobility model is needed, in which can accurately reflect the analytical and simulation results with desired steady state speed and uniform spatial node distribution.

2.5.1. Random Waypoint Mobility Model

Random Waypoint mobility model is most widely used in MANETs studies because of its straightforward design and easy implementation [30]. However, RWP suffers from some deficiencies in its stationary behavior:

- The average speed of a node in RWP model decreases over time [31, 32].
- RWP mobility model does not produce a uniform spatial node distribution at the steady state and nodes are concentrated near the center of the simulated region [33, 34].

In the traditional random waypoint (RWP) mobility model, each node of the network is assigned an initial location (X_0, Y_0), and a destination point (waypoint) (X_1, Y_1), independently sampled from a random uniform distribution. A node moves from the initial location to the destination point with a constant speed v along straight line. Figure 2.13 shows the movement trace of a node using RWP mobility model within a bounded area. The movement of each node is linear but a node reflects and changes its direction sharply when it approaches the boundary. The speed is chosen randomly from a uniform distribution with minimum and maximum speed $[V_{min}, V_{max}]$, where V_{min} = 0 and V_{max} is the maximum allowable node speed. Once the node reaches its destination, it rests for a predefined pausing time and then chooses a new random

destination and speed. It repeats the whole procedure through the simulation period (refer to Chapter 3 for more details).

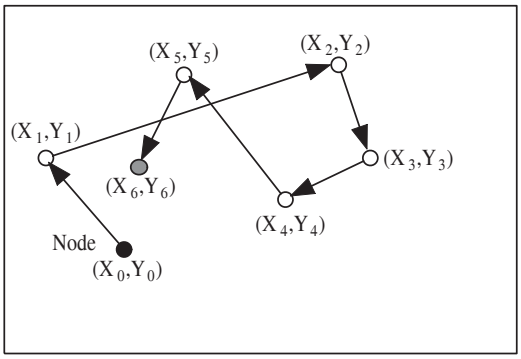

Figure 2.13. Node movement of random waypoint model.

2.5.2. Random Direction Mobility Model

Random direction (RD) mobility model was developed to alleviate the nodes' behavior in RWP mobility model. In this model, each node chooses a random direction $(0-180)$ instead of a random destination independently from a random uniform distribution. A node travels toward the simulation area border in that direction. Once the node reaches the boundary, it stops for a certain period of time and then selects a new random angular direction. The whole procedure is repeated independently through the simulation period [35]. This model forces nodes to travel to the boundary of the simulation area before changing direction and speed.

RD mobility model differs from purely stochastic models in which node destinations, speeds and pause times are selected from distributions derived from real data. Also, it captures the spatial and temporal dependencies between node movements. Moreover, this model has the advantage of being analytically tractable and captures a wide range of mobility patterns of nodes [36].

2.5.3. Random Walk Mobility Model

Random walk (RW) mobility model is based on random directions and speeds, in which the speed and direction are changed at discrete time intervals. It is known as brownian motion model and was originally proposed to emulate the movement behavior of particles in physics [25]. Also, it is a memoryless mobility model because the speeds of a node are independent for different step-lengths.

In RW mobility model, a mobile node selects a random step-length d sampled from a known distribution, speed v from a uniform distribution over $[V_{min}, V_{max}]$ and random direction ϕ chosen uniformly from $[0, 2\pi]$. A node moves in a direction ϕ for a distance d along straight line at a speed v. Upon the completion of the step-length, node pauses for some time t_p and starts the next step-length. The whole procedure is repeated for all nodes independently. Moreover, if a node hits the network boundary, it bounces back into the simulation area.

Chapter 3

GAMMA RANDOM WAYPOINT MOBILITY MODEL FOR WIRELESS AD-HOC NETWORKS

Mobility has a dramatic effect on the performance of MANETs which in turn affects the overall performance of MANETs in terms of efficiency, throughput, routing protocols, delay and capacity. A theoretical result is presented in [37] which shows that the capacity of the stationary ad-hoc networks does not scale with the networks' size. Contrary to the stationary ad-hoc scenario, analytical results are presented in [38], which show that the capacity of mobile ad-hoc networks can actually scale with the networks' size. Nodes in MANETs are assumed to move according to many different mobility models, which govern the movement behavior of nodes within the network. Hence, mobility models play a significant role in reflecting the true performance of the dynamically changing network topologies. The choice of mobility models has significant effect on the performance of MANETs routing protocols which can be found in [39, 40, 41, 42, 43]. The authors in [44] investigate and quantify the effects of various factors (node speed, node pause time, network size, number of traffic sources and routing protocol) on the overall performance of ad-hoc networks. The study uses RWP mobility model and shows that the nodes' speed affects control overhead and throughput, while the pause time does not. In [45], the impact of node mobility on distributed and mobility adaptive clustering (DMAC) was explored and the cost of maintaining the

DMAC clustering structures when nodes move according to RWP, Brownian motion and Manhattan mobility models were evaluated.

3.1. Traditional RWP Mobility Model

RWP is one of the simplest mobility models used in ad-hoc networks; the model describes the movement of nodes' behavior in the simulated area. However, the traditional RWP suffers from speed decay and may fail to provide a steady state in that the average speed of nodes are consistently decreasing over time [46, 47]. Furthermore, the node speed distribution at the steady state may be different from the initial uniform distribution chosen at the beginning of simulation. To overcome the speed decay problem, the data collected from the initial sequence observation period of the simulation time are discarded to ensure the system has entered the steady state [48]. However, it is difficult to determine the duration of the initial period of the simulation because the convergence time may exceed the simulation period.

RWP mobility model does not produce a uniform node distribution in the network. Instead, the nodes are concentrated near the center of the simulated region in which the nodes keep in moving [34]. This is because nodes traveling between uniformly chosen points spend more time near the center than near the boundary. Furthermore, the average instantaneous node speed (average speed of all nodes at a given time) is shown to decrease over time. In [49], it is mathematically proven that RWP model does not produce a uniform node distribution in the network, where nodes are concentrated near the center of the simulated area due to the boundary effect. Extensive studies of the boundary effect are presented in [50]. A random direction model is proposed in [51] to eliminate the boundary effect problems. It is pointed out that the boundary

effect causes a non-uniform node distribution and fluctuation of node' density over time.

3.2. Mobility Characteristics

RWP is a general mobility model designed to model the mobility patterns for MANETs, where each node moves independently of others nodes and moves freely in the simulated area without obstructions. Therefore, RWP does not capture the mobility characteristics of spatial dependence of movement among nodes, temporal dependence of movement of a node over time and geographic restrictions. In contrast to RWP mobility model, Manhattan model is an urban traffic mobility model designed to model the mobility patterns for vehicular ad-hoc networks (VANETs). It's a map-based model that captures the movement pattern of nodes traveling on urban roads. Manhattan mobility model has high spatial dependence, high temporal dependence and imposes geographic restrictions on node mobility [52]. The main differences between RWP and Manhattan model are the following: In RWP, speed of a node is independent from other nodes, the speeds at two different time slots are independent and each node moves freely anywhere in the simulated area without obstructions. While in Manhattan mobility model, speed of a node is restricted by any preceding nodes' speed on the same lane, the speed of a node at a time slot is temporally dependent on the speed of the previous time slot and each node is restricted to a lane in the road.

The general approach of the existing research on mobility models focused on nodes' distribution within the simulated area and epoch lengths. The choice for velocity distribution is usually not studied carefully even though it is a challenging problem and has a significant effect in the accuracy of mobility models. Extensive studies of the

stochastic properties of RWP mobility model and the effects of mobility models on the spatial distribution are presented in [53, 54, 55, 56, 57, 58].

3.3. Speed Distribution of RWP Models

The most common problem with simulation studies using RWP model is the poor choice for the velocity distribution. Such velocity distributions may lead to a situation of stationary state, where each node stops moving, e.g., uniform distribution $(U \sim [0, V_{max}])$ [59]. The study in [60], derives the stationary distribution of speed and initializes the mobility state to a sample drawn from the steady state uniform distribution. A method is proposed in [61] to force the distribution of nodes to be uniform and remove any artifacts in simulation results which may arise due to nodes crowding in the center of the simulation area. This is achieved by making the pause time of the nodes dependent on their pause location.

3.3.1. Uniform Speed Distribution

The node's speeds in the traditional RWP model are sampled from uniform distribution $[V_{min}, V_{max}]$, where $V_{min} = 0$, the given analytical model is drawn in [31]. Then the pdf of the nodes' speed V is

$$f_V(v) = \frac{1}{V_{max} - V_{min}} \qquad V_{min} \leq v \leq V_{max}. \tag{3.1}$$

all nodes have $V_{max} = V_{min} = 0$ at $t = 0$.

The pdf of the travel time t is given by:

$$f_T(t) = \begin{cases} \frac{2t}{3d_{max}^2} - (V_{max}^2 + V_{min}^2 + V_{max}V_{min}) & 0 \leq t \leq \frac{d_{max}}{V_{max}} \\ \frac{2d_{max}}{3t^2(V_{max}-V_{min})} - \frac{2tV_{min}^3}{3d_{max}^2(V_{max}-V_{min})} & \frac{d_{max}}{V_{max}} \leq t \leq \frac{d_{max}}{V_{min}} \\ 0 & t \geq \frac{d_{max}}{V_{min}}. \end{cases} \quad (3.2)$$

The expected traveling time is

$$E[t] = \frac{2d_{max}}{3\left(V_{max} - V_{min}\right)} - \ln\left(\frac{V_{max}}{V_{min}}\right). \quad (3.3)$$

The average steady state speed for a given node is given as follows

$$E[V_{ss}] = \frac{V_{max} - V_{min}}{\ln\left(\frac{V_{max}}{V_{min}}\right)}. \quad (3.4)$$

In traditional RWP mobility model, speeds of nodes are chosen from a uniform distribution $[0, V_{max}]$. Therefore, when $V_{min} = 0$ in (4.3) and (3.4), then $E[t] \rightarrow \infty$ and $E[V_{ss}] \rightarrow 0$, respectively. The authors in [31] proposed to set a non-zero minimum speed to resolve the fast decay of speed. This modified RWP mobility model outperforms the original RWP model as shown in Chapter 6.

3.3.2. Clipped Normal Speed Distribution

The node's speeds are sampled from clipped normal distribution (i.e., one that is distributed between finite maximum and minimum values). In addition, the expected values of the steady-state speed distribution with and without pausing time were de-

rived in [62]. A node always starts from a moving state whether there is pause or no pause time. Therefore, the reference of the initial average speed is taken from a move state. The initial probability density function of the clipped normal is given by:

$$f_V(v) = \frac{1}{K\sqrt{2\pi\sigma^2}}\, e^{-\frac{(v-\mu)^2}{2\sigma^2}} \qquad V_{min} \leq v \leq V_{max}, \tag{3.5}$$

where σ is the standard deviation, $\mu = \frac{V_{min}+V_{max}}{2}$ and K is the normalized constant is given by:

$$K = \int_{V_{min}}^{V_{max}} \frac{1}{\sqrt{2\pi\sigma^2}}\, e^{-\frac{(v-\mu)^2}{2\sigma^2}}\, dv.$$

The pdf of the steady state speed without pausing time is

$$f_{V_{ss}}(v) = \frac{\frac{1}{v}\, e^{-\frac{(v-\mu)^2}{2\sigma^2}}}{\int_{V_{min}}^{V_{max}} \frac{1}{v'}\, e^{-\frac{(v'-\mu)^2}{2\sigma^2}}\, dv'}. \tag{3.6}$$

The expected value of the steady state speed without pausing time is

$$E[V_{ss}] = \frac{1}{\int_{V_{min}}^{V_{max}} \frac{1}{v}\, \frac{1}{K\sqrt{2\pi\sigma^2}}\, e^{-\frac{(v-\mu)^2}{2\sigma^2}}\, dv}. \tag{3.7}$$

The pdf of the steady state speed with pausing time is

$$f_{V_{ss}}(v) = \frac{\frac{1}{v}\, e^{-\frac{(v-\mu)^2}{2\sigma^2}}}{\int_{V_{min}}^{V_{max}} \frac{1}{v'}\, e^{-\frac{(v'-\mu)^2}{2\sigma^2}}\, dv'}\, P_{move}. \tag{3.8}$$

The expected value of the steady state speed with pausing time is

$$E[V_{ss}] = \frac{\frac{d_{max}}{2}}{\frac{d_{max}}{2} \int_{V_{min}}^{V_{max}} \frac{1}{v}\, \frac{1}{K\sqrt{2\pi\sigma^2}}\, e^{-\frac{(v-\mu)^2}{2\sigma^2}}\, dv + \frac{t_{p(max)}}{2}}, \tag{3.9}$$

where P_{move} is the probability that a node is in a move state and is given as follows

$$P_{move} = \frac{\frac{d_{max}}{2} \int_{V_{min}}^{V_{max}} \frac{1}{v}\, \frac{1}{K\sqrt{2\pi\sigma^2}}\, e^{-\frac{(v-\mu)^2}{2\sigma^2}}\, dv}{\frac{d_{max}}{2} \int_{V_{min}}^{V_{max}} \frac{1}{v}\, \frac{1}{K\sqrt{2\pi\sigma^2}}\, e^{-\frac{(v-\mu)^2}{2\sigma^2}}\, dv + \frac{t_{p(max)}}{2}}. \tag{3.10}$$

3.3.3. *Beta(2,2)* Speed Distribution

The node's speed are sampled from $Beta(2,2)$ distribution. This is because the $Beta(2,2)$ function does not change the RWP main features and this distribution can be readily incorporated into network simulators. The analytical and simulation results drawn in [63] show that this model can stabilizes the instantaneous average speeds of nodes (zero pause time is considered). The pdf of speed distribution $Beta(2,2)$ is given as follows

$$f_V(v) = -\frac{6\left(v - \frac{V_{max}+V_{min}}{2}\right)^2}{(V_{max}-V_{min})^3} + \frac{3}{2\,(V_{max}-V_{min})}. \tag{3.11}$$

The time average of the steady state speed without pausing time is

$$E[V_{ss}] = 2\left(V_{max} - V_{min}\right)^3 \left[\frac{2C}{V_{max}^3} - 12V_{max}V_{min}\ln\left(\frac{V_{max}}{V_{min}}\right) + \frac{27}{5}\left(V_{max}^2 - V_{min}^2\right) + \left(V_{max} - \frac{3}{5}V_{min}\right)\left(V_{min} - \frac{V_{min}^4}{V_{max}^3}\right)\right]^{-1}, \tag{3.12}$$

where C is constant and is given by

$$C = -\frac{6}{5}\left(V_{max}^5 - V_{min}^5\right) + \frac{3}{2}\left(V_{max} + V_{min}\right)\left(V_{max}^4 - V_{min}^4\right) - 2V_{max}V_{min}\left(V_{max}^3 - V_{min}^3\right),$$

this is for $V_{min} \leq v \leq V_{max}$ and $0 < V_{min} < V_{max}$. It also shows that

$$E[V_{ss}] = \lim_{V_{min}\to 0} E[V_{ss}] = \frac{V_{max}}{3}$$

To ensure a realistic mobility model that relies on more precise distribution of the nodes' speed and give an accurate movement of nodes, a careful study is needed to determine the node speed distribution and the behavior of nodes' mobility in the network environment. In this study, we model the nodes' speed of the RWP model for MANETs. In particular, we derive the probability distribution and the expected value of the steady state speed. This study is important in evaluating precisely the performance of MANETs (e.g., throughput, connectivity, routing, delay and capacity, etc.).

3.4. Stochastic Properties of RWP Model

In this model, it is assumed that each node moves independent of other nodes within the network and all nodes have the same stochastic movement properties. The asymptotic spatial distribution of a single node is the same as the asymptotic distribution of all nodes. Considering a single node, let $L_j^i(t)$ represent the waypoint location of node i at time t, $L_j^i(t) = [X_j(t), Y_j(t)]$, where $j = 0, 1, 2, ..., K$ is the motion step. $L_j's$ are independent and identical distributed (iid) random variables, uniformly distributed over a deployment region.

By definition, random waypoints of node $L_j's$ are independent, but the distances between these random points $d_{j,j+1}$ are stochastically dependent. The authors in [34] noted that the independent random point (IRP) process and the RWP process shared several statistical properties. As defined by stochastic process, they show the mean-ergodic property of the RWP mobility model, i.e., statistically there is no difference between sampling repeatedly from a single random variable or successively from a sequence. This ergodicity property implies that the analysis of determining the expected distance of RWP mobile node can be simplified by considering only the distance between two points placed uniformly at random in a deployment region. Let us define $d_{j,j+1}(t)$ as the path length which is the distance from the initial location to the waypoint destination at time t (distances between two consecutive random waypoints).

$$\begin{aligned} d_{j,j+1}(t) &= \parallel L_{j+1}(t) - L_j(t) \parallel, \\ &= \sqrt{|X_{j+1}(t) - X_j(t)|^2 + |Y_{j+1}(t) - Y_j(t)|^2}. \end{aligned} \tag{3.13}$$

The remoteness of the waypoint destination from the initial location of node i at time t is define as the cumulative density function of distance; $R_i(t) = F(d_{j,j+1}(t))$. As a node moves, the remoteness of waypoint destination changes in time, while the traveling speed remains constant along the path length. The instantaneous average node speed at time t is given by:

$$\bar{v}(t) = \frac{1}{N} \sum_{i=1}^{N} v_i(t). \tag{3.14}$$

$$v_i(t) = \frac{1}{K} \sum_{j=0}^{K-1} \left| \frac{d}{dt} d_{j,j+1}(t) \right|, \tag{3.15}$$

where $v_i(t)$ is the speed of node i at time t and N is the total number of nodes.

If nodes' speed is chosen from a random distribution $f_V(v)$ at each waypoint, each node travels at a constant speed v during one transition period along a straight line d. Then the transition traveling time $t = d/v$ provided that $V_{min} \leq v \leq V_{max}$ and $V_{min} > 0$. The expected traveling time is $E[t] = E[d]E[1/v]$, where v and d are independent random variables. According to the theory of geometric probability, the expected distance between two random points uniformly distributed on a square of side r, $E(d) = 0.521405\, r$ [64]. Since speed is assumed to be independent of distance, the probability density function of nodes' speed $f_V(v)$ will depend on $E[d]/v$. Furthermore, since $E[d]$ is constant, $f_V(v)$ will be proportional to $1/v$.

The random variable t is a function of two random variables d and v and is given by $t = g(d, v)$. Since v and d are independent random variables, their joint pdf can be written as $f_{DV}(d, v) = f_D(d) f_V(v)$. Then the expected traveling time can be obtained in terms of the joint pdf [65]:

$$\begin{aligned} E[t] &= E[g(d,v)] = \iint_{-\infty}^{\infty} g(d,v)\, f_{DV}(d,v)\, dd\, dv, \\ &= E[d] \int_{V_{min}}^{V_{max}} \frac{1}{v}\, f_V(v)\, dv. \end{aligned} \tag{3.16}$$

By using the inverse transformation method for finding the cumulative distribution function of the traveling time, $F_T(t)$ is computed by using figure 3.1:

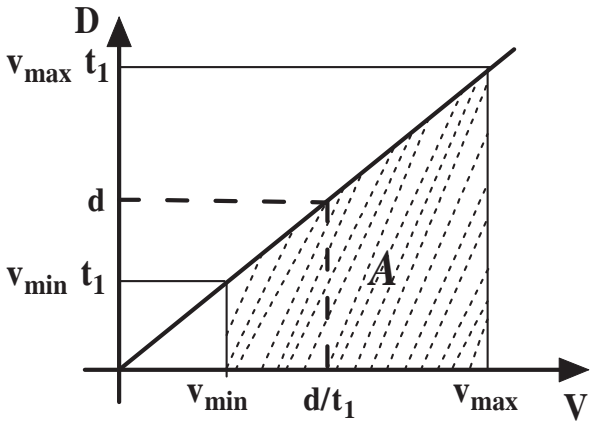

Figure 3.1. Derivation of the pdf of traveling time $f_T(t)$.

$$
\begin{aligned}
F_T(t) &= P\{T \le t\} = P\{d \le vt_1\} \\
&= \int_A f_{DV}(d,v)\, dv\, dd = \int_A f_D(d)\, f_V(v)\, dv\, dd,
\end{aligned}
$$

where

- $0 < d < V_{min}t_1 \qquad V_{min} > \dfrac{d}{t_1}, \qquad v : V_{min} \to V_{max}$
- $V_{min}t_1 \le d \le V_{max}t_1 \qquad V_{min} \le \dfrac{d}{t_1},\ V_{max} \ge \dfrac{d}{t_1}, \quad v : V_{min} \to V_{max}$
- $d < 0,\ d > V_{max}t_1 \qquad V_{max} < \dfrac{d}{t_1}, \qquad v \to 0$

$$
\begin{aligned}
&= \iint_{0<d<V_{min}t_1} f_{DV}(d,v)\, dv\, dd + \iint_{V_{min}t_1 \le d \le V_{max}t_1} f_{DV}(d,v)\, dv\, dd, \\
&= \int_0^{V_{min}t_1} \int_{V_{min}}^{V_{max}} f_{DV}(d,v)\, dv\, dd + \int_{V_{min}t_1}^{V_{max}t_1} \int_{V_{min}}^{V_{max}} f_{DV}(d,v)\, dv\, dd, \\
&= \int_0^{V_{max}t_1} \int_{V_{min}}^{V_{max}} f_{DV}(d,v)\, dv\, dd \\
&= \int_0^{V_{max}t_1} f_D(d) \int_{V_{min}}^{V_{max}} f_V(v)\, dv\, dd. \qquad (3.17)
\end{aligned}
$$

Taking the derivative of (3.17) with respect to time to find the pdf of traveling time,

$$
f_T(t) = \begin{cases} \int_{V_{min}}^{V_{max}} v\, f_D(tv)\, f_V(v)\, dv, & 0 \le t \le t_{max} \\ \\ 0, & \text{otherwise}, \end{cases} \qquad (3.18)
$$

where $t_{max} = \frac{d_{max}}{V_{min}}$.

The expected steady state speed for a given node (see APPENDIX 2) can be obtained

as follows [31]:

$$\begin{aligned} E[V_{ss}] &= \lim_{T\to\infty} \frac{1}{T} \int_0^T v(t)\, dt \\ &= \frac{E[d]}{E[t] + E[t_p]}, \end{aligned} \tag{3.19}$$

where V_{ss} is the steady state speed, $v(t)$ is the instantaneous node speed at time t and $E[t_p]$ is the expected pausing time.

The expected value of the steady state speed can be obtained also in terms of the nodes' speed v and probability density function of steady state speed $f_{V_{ss}}(v)$ as follows

$$E[V_{ss}] = \int_{V_{min}}^{V_{max}} v\, f_{V_{ss}}(v)\, dv. \tag{3.20}$$

The probability density function of the steady state speed $f_{V_{ss}}(v)$ is given by

$$f_{V_{ss}}(v) = \frac{1/v\, f_V(v)}{E[1/v]}. \tag{3.21}$$

The dynamic state for the distribution of node location $f_{X,Y}(x, y)$, is composed of two distinct component states, pause and mobility state. The probability density function of node's location is given by [34]:

$$f_{X,Y}(x, y) = f_p(x, y) + f_m(x, y). \tag{3.22}$$

The pause state for the distribution of node location $f_p(x, y)$ accounts for the time that

a node pauses at the destination waypoint before starting a new movement period. The mobility component state for the distribution of node location $f_m(x, y)$ accounts for the time that a node is actually traveling between two points. The pausing time t_p of a node is defined as the ratio of the average pausing time $E[t_p]$ and the average of one cycle (average pausing time period $E[t_p]$, and average traveling time period between two pauses $E[t]$). Hence, $E[t_p]$ is given by

$$E[t_p] = \frac{t_p}{1 - t_p} E[t]. \tag{3.23}$$

The expected pausing time can be obtained also in terms of nodes' pausing time t_p and probability density function of pausing time $f_{T_p}(t_p)$ as follows:

$$E[t_p] = \int_{T_{p(min)}}^{T_{p(max)}} t_p \, f_{T_p}(t_p) \, dt_p. \tag{3.24}$$

3.5. Gamma Random Waypoint Model

The speed distribution has an impact on mobility model's steady state. Therefore, speed should be chosen from a distribution to precisely model its variations. In this mobility model, each node chooses initial location (X_0, Y_0) and destination point (X_1, Y_1) independently from a random uniform distribution on the unit square. A node moves toward its destination point with a constant speed v along a straight line. The speed is chosen randomly in the interval of $[V_{min}, V_{max}]$ and sampled from Gamma distribution. Once the node reaches its destination, it selects a new random destination and speed. The whole procedure is repeated independently through the simulation period. The simulation model is summarized by the following steps:

(1) Generate the nodes' locations (X_0, Y_0) and (X_1, Y_1) independently from a random uniform distribution;

(2) Compute the traveling distance, $d = \sqrt{|X_{j+1}(t) - X_j(t)|^2 + |Y_{j+1}(t) - Y_j(t)|^2}$;

(3) Generate the nodes' speed randomly in the interval of $[V_{min}, V_{max}]$ and sampled from Gamma distribution;

(4) The node travels to (X_1, Y_1) at the initially chosen speed. Upon reaching (X_1, Y_1), new random speeds and destinations are chosen from the designated distribution.

Gamma distributions have been used for random modeling in many fields. The Gamma distribution is employed in the proposed model in order to represent the distribution of nodes' speed. Gamma distribution has the shape parameter α and the scale parameter β. The Gamma probability density function with parameters α and β is given by:

$$f(v|\alpha, \beta) = \frac{1}{\beta^{\alpha}\,\Gamma(\alpha)}\, v^{\alpha-1}\, e^{-v/\beta}, \quad v,\ \alpha \text{ and } \beta > 0, \tag{3.25}$$

for large values of α, the distribution of nodes' speed is closely approximated by Gaussian distribution, except for the fact that Gamma distribution density is defined for positive values only. The Gamma cumulative distribution function is given by:

$$F(v|\alpha, \beta) = \frac{1}{\beta^{\alpha}\,\Gamma(\alpha)} \int_0^v \tau^{\alpha-1}\, e^{-\tau/\beta}\, d\tau, \tag{3.26}$$

for $v > 0$, $\Gamma(\alpha, \beta)$ distribution has a mean $\alpha\beta$ and variance $\alpha\beta^2$. The standard deviation is proportional to β and when $\alpha > 1$ and Gamma mode m = 1, $\beta = \frac{1}{\alpha-1}$. When

$\beta = 1$, the functions are identical.

3.5.1. GRWP Mobility Model without Pausing

Pause time is the duration of time at the destination waypoint, and is set to zero to indicate continuous mobility. Once the node reaches its destination, it selects a new random destination and speed independent of all other nodes in the network. Using the Gamma distribution of (3.25) in (3.21), the pdf of the steady state speed becomes

$$\begin{aligned} f_{V_{ss}}(v) &= \frac{\frac{1}{v}\,\frac{1}{\beta^{\alpha}\,\Gamma(\alpha)}\,v^{\alpha-1}\,e^{-v/\beta}}{\int_{V_{min}}^{V_{max}} \frac{1}{v}\,\frac{1}{\beta^{\alpha}\Gamma(\alpha)}\,v^{\alpha-1}\,e^{-v/\beta}\,dv}, \\ &= \frac{v^{\alpha-2}\,e^{-v/\beta}}{\int_{V_{min}}^{V_{max}} v^{\alpha-2}\,e^{-v/\beta}\,dv}, \end{aligned} \tag{3.27}$$

Simplifying (3.27), the pdf of the steady state speed can be obtained as follows (see APPENDIX 4):

$$\begin{aligned} f_{V_{ss}}(v) &= \frac{v^{\alpha-2}\,e^{-v/\beta}}{e^{-v/\beta}\sum_{k=0}^{\alpha-2}\frac{(-1)^k\,(\alpha-2)!\,v^{\alpha-k-2}}{(\alpha-k-2)!\,(-1/\beta)^{k+1}}}\Bigg|_{V_{min}}^{V_{max}}, \\ &= \frac{v^{\alpha-2}}{\beta^{\alpha-1}\,(\alpha-2)!\sum_{n=0}^{\alpha-2}\frac{(v/\beta)^n}{n!}}\Bigg|_{V_{max}}^{V_{min}}. \end{aligned} \tag{3.28}$$

Recalling (5.13) and Substituting the pdf of Gamma distribution (3.25), the expected

value of the steady state speed without the pausing time becomes

$$\begin{aligned} E[V_{ss}] &= \int_{V_{min}}^{V_{max}} v\, f_{V_{ss}}(v)\, dv = \int_{V_{min}}^{V_{max}} \frac{f_V(v)}{E[1/V]}\, dv, \\ &= \int_{V_{min}}^{V_{max}} \frac{\frac{1}{\beta^\alpha\, \Gamma(\alpha)}\, v^{\alpha-1}\, e^{-v/\beta}}{\int_{V_{min}}^{V_{max}} \frac{1}{v}\, \frac{1}{\beta^\alpha\, \Gamma(\alpha)}\, v^{\alpha-1}\, e^{-v/\beta}\, dv}\, dv, \\ &= \int_{V_{min}}^{V_{max}} \frac{v^{\alpha-1}\, e^{-v/\beta}}{\int_{V_{min}}^{V_{max}} v^{\alpha-2}\, e^{-v/\beta}\, dv}\, dv, \end{aligned} \tag{3.29}$$

applying the numerical integration of (3.29) to find the expected value of the steady state speed. V_{min} = 1 m/sec, V_{max} = 19 m/sec, $\alpha = \frac{V_{min}+V_{max}}{2}$ = 10 and β = 1, resulting $E[V_{ss}]$ = 8.95 m/sec.

3.5.2. GRWP Mobility Model with Pausing

After reaching the destination waypoint, the node stops for a duration of pause time t_p chosen from uniform distribution in the interval $[t_{p,min}, t_{p,max}]$, and then selects a new random destination and speed for the next movement period. The expected value of pause time becomes $E[t_p] = \frac{t_{p,min}+t_{p,max}}{2}$ or can be computed from (5.17) or (3.24). The expected traveling time can be computed by substituting (3.25) in (3.16) as follows:

$$\begin{aligned} E[t] &= E[d] \int_{V_{min}}^{V_{max}} \frac{1}{v}\, \frac{1}{\beta^\alpha \Gamma(\alpha)}\, v^{\alpha-1}\, e^{-v/\beta}\, dv, \\ &= \frac{E[d]}{\beta^\alpha\, \Gamma(\alpha)} \int_{V_{min}}^{V_{max}} v^{\alpha-2}\, e^{-v/\beta}\, dv. \end{aligned} \tag{3.30}$$

Simplifying (3.30), the expected traveling time can be obtained as (APPENDIX 5):

$$\begin{aligned} E[t] &= \frac{E[d]}{\beta^{\alpha}\,\Gamma(\alpha)}\, e^{-v/\beta} \sum_{k=0}^{\alpha-2} \frac{(-1)^k\,(\alpha-2)!\,v^{\alpha-k-2}}{(\alpha-k-2)!\,(-1/\beta)^{k+1}} \Bigg|_{V_{min}}^{V_{max}}, \\ &= \frac{E[d]}{\beta(\alpha-1)}\, e^{-v/\beta} \sum_{n=0}^{\alpha-2} \frac{(v/\beta)^n}{n!} \Bigg|_{V_{max}}^{V_{min}}. \end{aligned} \tag{3.31}$$

Substituting (3.31) in (3.19), after further simplification of terms, the expected value of the steady state speed with pausing time becomes

$$E[V_{ss}] = \frac{1}{\dfrac{e^{-v/\beta}}{\beta(\alpha-1)} \left[\sum_{n=0}^{\alpha-2} \dfrac{(v/\beta)^n}{n!}\right] + \dfrac{E[t_p]}{E[d]}} \Bigg|_{V_{max}}^{V_{min}}, \tag{3.32}$$

applying the numerical computation of (3.32) to find the expected value of the steady state speed with pausing time. V_{min} = 1 m/sec, V_{max} = 19 m/sec, $t_{p(min)}$ = 0 sec, $t_{p(max)}$ = 60 sec, α = 10 m/sec and β = 1, resulting $E[V_{ss}]$ = 5.95 m/sec.

Chapter 4

EFFECT OF MOBILITY MODEL ON THE IEEE 802.11 RTS/CTS

MANET is a form of wireless ad-hoc networks consists of wireless mobile nodes forming a temporary network. These networks are momentary in nature, high flexible, fast established and self-reconfigured. However, wireless network without a fixed infrastructure and with nodes' mobility enabled, the networks' topology keeps on changing. This causes frequent path changes and leads to increase the network congestion and transmission delay over the network. Moreover, if the nodes in the network are heterogeneous, then the connection topology is asymmetric because the transmission power of a node pair is different from each other.

Multi-hop wireless ad-hoc networks provide flexible solutions to applications where wireless nodes can communicate with each other without a fixed wired infrastructure. The multi-hop ad-hoc wireless networks allow quick deployment of the networks and allow nodes to expand the network coverage area. In addition, it provides flexibility and robustness to the networks because of its dynamic capability nature of forming a network. Broadcast transmission is one of the significant characteristics of wireless ad-hoc networks. A group of nodes may contend to access the transmission medium at the same time resulting in possible collisions. The transmission medium in wireless ad-hoc network is shared by multiple wireless nodes in the network. Thus, the MAC

protocol is needed to coordinate and regulate the medium access efficiently and fairly among all nodes otherwise a high collision rate may result in the network. The limited bandwidth medium of the wireless ad-hoc networks, packet overhead, hidden and exposed terminal problems contribute to throughput network limitation.

Although the IEEE 802.11 based wireless multi-hop ad-hoc networks promise high performance and cost effective deployments. The wireless networks suffer from packet corruption and collisions due to error-prone wireless channels and transmission interference on the shared medium. However, the RTS/CTS collision mechanism is not able to handle the complex collision situations in multi-hop ad-hoc networks effectively, where hidden nodes exist [66, 67]. The RTS/CTS functionality affects the protocol in the following ways:

1. It expends more bandwidth by transmitting two additional control packets per data packet transmission.

2. It increases bandwidth efficiency by reducing the collision probability. They are coordinated through a distributed collision avoidance mechanism. Collisions that do occur are of small control frames, not of data frames.

3. In certain cases, it decreases bandwidth efficiency because it reserves time space for its transmission, where or when it might actually not be necessary. However, to alleviate the imposed overhead, the usage of RTS/CTS is dynamically determined according to the transmitted packet payload size.

Most of the research on the IEEE 802.11 DCF model assume a single-hop network with bounded packet transmission probability and network throughput under the condition of traffic saturation using analytical model [68, 69, 70]. The authors in [71] analyze the goodput of IEEE 802.11 DCF in ring and mesh topologies using a multi-hop network. Existing traditional MAC protocols for ultra-wide band (UWB) are either based on mutual exclusion (other transmissions are not allowed within the same collision region) or on a combination of power control and mutual exclusion [72, 73, 74, 75]. Based on mathematical analysis, The authors in [76] proposed MAC protocol to increase the network throughput. They proposed an optimal MAC protocol, in which an interfering source node can transmit simultaneously to its destination as long it is outside the defined exclusion region of other destination nodes. In contrast, interference inside the exclusion region should be controlled (no other transmissions are allowed within the exclusion region).

4.1. Access Scheme of the MAC Protocol

A node that intends to transmit and senses the medium as an idle for an interval longer than the DIFS time, it can start its own transmission. If the medium is sensed busy, this node chooses a random backoff time that is randomly chosen within its current contention window CW size, and initialize the backoff timer whenever the medium is sensed as idle. The node freezes the countdown of its backoff timer whenever it senses the medium busy. This implies that the node should wait for the completion of other nodes' transmissions without counting down its backoff timer. When the medium is sensed idle again, it resumes the remainder of the backoff timer. When the backoff time becomes zero, the node sends its packet after a DIFS interval time. Backoff time or

CW is an integer number measured in time slots and uniformly chosen in the interval $(0, CW - 1)$. At the first transmission attempt, CW size equals its minimum value CW_{min} and it is doubled at each retransmission attempt up to maximum $CW_{max} = 2^m CW_{min}$ value and resets its CW to CW_{min} after every successful transmission, where m is the maximum backoff stage. Typical values of CW_{min} and CW_{max} are 32 and 1024 slots respectively [77]. More Backoff schemes are presented in [78, 79, 80]. CSMA/CA scheme employs the BEB to ensure stability of the backoff process. Collisions can take place only when two nodes select the same slot, and the collisions of 802.11 RTS/CTS access mechanism can occur only on RTS frames.

In the RTS/CTS mechanism, the source node transmits an RTS after gaining an access over the medium, the RTS contains the frame duration information. If the destination node is capable of receiving the packet, it responds with a CTS control packet that also carries the frame duration after waiting a period of time equal to the SIFS time. If any node captures the RTS packet while it is not the destination of the RTS packet, it waits until it captures the corresponding CTS. If it does not receive CTS, then the node realizes that it does not interfere with the transmission at the receiver and is free to proceed with its transmission sequence. On the other hand, if a node receives CTS then it defers its own transmissions for the duration of the packet transmission. In the case where the node receives only CTS packet, this means that the node is out of the transmission range of the source node but within the transmission range of the destination node. Therefore, the node must remain silent for the specified duration of the packet transmission. This guarantees that all nodes within the range of either source or destination are aware of the ongoing transmissions along with their duration.

In analyzing the performance of CSMA/CA with respect to the assumption of [14], the author estimates the saturation throughput based on two-dimensional Markov chain, where nodes always have packets to transmit. Probability of transmission is given as follows

$$\begin{aligned} P_{tr} &= P(k \geq 1) = 1 - P(k = 0) \\ &= 1 - (1 - p)^n, \end{aligned} \tag{4.1}$$

where p is the probability that a node transmits a packet randomly in a generic slot time and k is the transmission attempt, transmission takes place when backoff counter reaches zero. $(1 - p)^n$ is the probability of zero transmission in the given slot time.

The probability that a transmitted packet collides P_c (the probability that at least one out of $n-1$ remaining nodes transmits in the given time slot) is assumed to be constant and independent of the previous transmission. This collisions' probability is seen by the transmitted packet and is given by:

$$P_c = 1 - (1 - p)^{n-1}, \tag{4.2}$$

where $(1-p)^{n-1}$ is the joint probability that $n-1$ nodes out of n nodes do not transmit a packet. Expressing p in term of P_c and contention windows (CW)

$$p = \frac{2(1 - 2P_c)}{(1 - 2P_c)(CW + 1) + P_c CW(1 - (2P_c)^m)}, \tag{4.3}$$

where m is the number of backoff stage. At the first transmission attempt, CW size equals its minimum value $CW = CW_{min}$ and it is doubled at each retransmission attempt up to maximum value $CW_{max} = 2^m W$. Collisions can take place only when two nodes select the same slot (during a contention procedure). Furthermore, the successful and collision transmissions of IEEE 802.11 RTS/CTS access mechanism are given by:

$$\begin{aligned} T_s &= T_{RTS} + T_{CTS} + T_D + T_{ACK} + DIFS + 3SIFS + 4\tau \\ T_c &= T_{RTS} + DIFS + \tau, \end{aligned} \tag{4.4}$$

where T_s and T_c are the average time that the medium is sensed to be busy due to successful and collision transmission, respectively. T_D is the payload transmission time including MAC and physical header and τ is the propagation delay. T_{RTS}, T_{CTS}, and T_{ACK} are the transmission time of the control packets RTS, CTS, and ACK, respectively.

Probability of successful transmission P_s is defined as the probability of no collision, which is given by the probability that exactly one transmission attempt, conditional that there is at least one transmission attempt in the given slot time.

$$\begin{aligned} P_s &= P\left[k = 1 \mid k \geq 1\right] \\ &= \frac{P\left[k \geq 1 \mid k = 1\right] P(k = 1)}{P(k \geq 1)} = \frac{np(1-p)^{n-1}}{1 - P(k = 0)} \\ &= \frac{np(1-p)^{n-1}}{1 - (1-p)^n}. \end{aligned} \tag{4.5}$$

Throughput S is defined as the ratio of the average time for successful payload transmission and the average length of one cycle time. The average time of successful transmitted payload, $E[T_D] = P_s P_{tr} T_D$. The average busy time slots contain busy slots due to collision and successful transmissions, hence $E[T_{busy}] = P_{tr} P_s T_s + P_{tr}(1 - P_s)T_c$. The average idle time slots, $E[T_{idle}] = (1 - P_{tr})\delta_{idle}$, where δ_{idle} is the duration of idle slot time. S is given by [14]:

$$\begin{aligned} S &= \frac{E\left[T_D\right]}{E\left[\text{length of cycle time}\right]} \\ &= \frac{E\left[T_D\right]}{E[T_{busy}] + E[T_{idle}]} \\ &= \frac{P_s P_{tr} T_D}{P_{tr} P_s T_s + P_{tr}(1 - P_s)T_c + (1 - P_{tr})\delta_{idle}}. \end{aligned} \tag{4.6}$$

4.2. Distributed Coordination Function

DCF is the fundamental medium access method based on the CSMA/CA scheme with rotating backoff for the distributed medium sharing and it supports asynchronous data transfer. All nodes have equal probability of gaining access to the medium, where every node has to re-contend for the medium after every packet transmission. However, in time-sensitive applications, DFC does not guarantee a minimum access delay. In addition, the performance of DCF in multi-hop environments is far from optimal. This is because DCF was originally designed for centralized single-hop wireless networks. With the continuing development of wireless networks and the increased of spatial reuse of medium resources, the communication range of an individual node is reduced.

Most researches study the IEEE 802.11 model; assume single-hop 802.11 wireless networks. Usually they provide a bound for the packet transmission probability and

the network throughput in the condition of traffic saturation, where node always has packets ready for transmission [14, 81, 82, 83, 84]. Other studies considered multi-hop wireless networks are presented in [85, 86, 87]. The work in [88, 89] investigates the performance of RTS/CTS handshake mechanism with the presence of interference between nodes. For better performance of RTS/CTS and minimal interference between nodes, the interference range should be shorter than the transmission range. Also, The authors in [90, 91], proposed an adaptive setting mechanism to increase the performance of IEEE 802.11 RTS/CTS in the outdoor scenarios, where long distance links are not optimal in outdoor communications. Therefore, distance links between nodes should be controlled by using the carrier sensing threshold.

4.3. Network Model Scenarios

Throughput and delay in ad-hoc networks can be influenced by various factors such as network size, transmission range and node mobility. Furthermore, one of the main characteristic of wireless ad-hoc networks is that the networks' topology may not be known (i.e., stationary random network or sensor network) or the networks' topology keeps in changing (i.e., MANETs). In stationary random network, the transmission range of nodes should be small to minimize interference; this will result in a higher throughput compared to the long transmission range. However, in mobile network, mobility allows nodes to approach each other closely. This allows the use of short transmission ranges and direct transmission or 1-hop relay transmission.

4.3.1. Stationary Nodes with Relaying Network Model

Stationary nodes N are randomly and uniformly distributed in the network area, where each source node chooses a random destination independently. Moreover, every node acts simultaneously as a source, a destination or a relay for other source-destination pairs (multi-hop relaying scheme). The authors in [37] proposed a model to compute the network throughput of the stationary ad-hoc networks, where the transmission ranges of all nodes are assumed to be homogenous. Recall knuth's notation [92]: $f(n) = \Theta(g(n))$ means that $f(n) = O(g(n))$; $g(n) = O(f(n))$. The result shows that the throughput per source-destination pair is about $\Theta(1/\sqrt{N \log N})$ at a bit rate of 1 bit per second. It also shows that as the number of nodes increases per unit area, the throughput per source-destination pair decreases to approximately $1/\sqrt{N}$. This is the best performance can be achieved, even if nodes are optimally placed in a unit area, traffic patterns are optimally assigned and each transmission's range is optimally chosen. So far, the performance of the stationary ad-hoc network model is limited, this is because of long direct transmission range communications between nodes pairs are infeasible due to the excessive interferences. Therefore, most communication between neighbor nodes occurs at transmission range of order $1/\sqrt{N}$. As a result, each packet is being transmitted through many other relay nodes before reaching the destination and the number of hops in a typical route is of order $\sqrt{N}$.

4.3.2. Mobile Nodes without Relaying Network Model

The throughput of a stationary nodes goes to zero, this is because any transmitted packet has to pass through a number of relay nodes of scales $\sqrt{N}$. However, in mobile nodes without relaying, the throughput can be improved by allowing direct transmis-

sion only when ever source and destination nodes approach each other closely from time to time. It is impossible to achieve a throughput capacity of $\Theta(1)$ per source-destination pair.

4.3.3. Mobile Nodes with Relaying Network Model

In [93], authors proposed a model to compute the throughput of mobile wireless ad-hoc networks, a 2-hop relaying scheme is proposed as shown in figure 4.1. It shows that the proposed scheme can achieve a throughput capacity of $\Theta(1)$ per source-destination pair. This throughput remains constant as the number of nodes grows arbitrarily large. However, the strategy of choosing a short transmission range communication in mobile network scenario is inefficient. This is because the time fraction of two nodes to be in range is too small, of the order of $1/N$. Therefore, the efficient strategy of communications in mobile wireless ad-hoc network scenario if the destination node is out of range; is that each source node broadcasts its packet stream to its neighbor nodes. These nodes keep in moving and serve as node relays and whenever they are in range with the destination node, they transmit the packet to the destination node.

4.4. Network Connectivity

Network connectivity is measured in term of connectivity ratio of nodes in the network, which is defined as the ratio of connected pair nodes and the total number of pairs in the network. According to the algorithm in [94], as the average speed increases the connectivity ratio drops rapidly. When the transmission range is 20 m, the delivery ratio is improved significantly under mobility of 1 - 40 m/sec. The algorithm has almost 100% connectivity ratio with a transmission range of 100 m and high mobility of 160

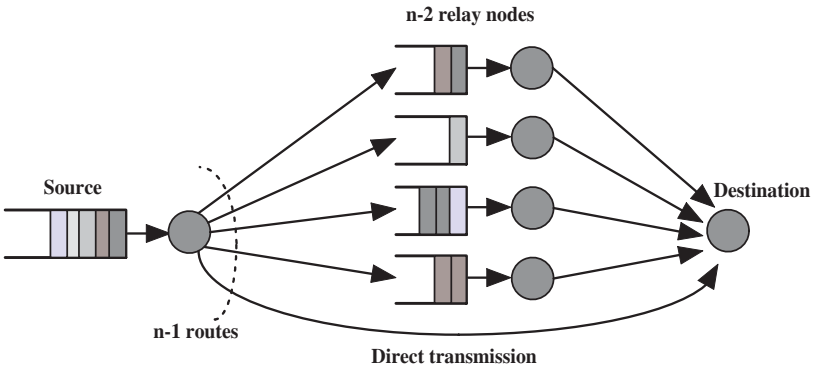

Figure 4.1. Scheduling policy of packet transmissions from source to relays or to destination [93].

m/sec. Each node maintains a list of the reachable neighbors that is updated periodically. This is to successfully receive an interference-free transmission. The density is defined as the average number of neighbors in the simulated area; this depends on the network size and the fraction of the covered transmission area and the entire simulated area:

$$N_{nbr} = \frac{\pi R^2}{A} N. \tag{4.7}$$

where N is the number of nodes in the simulated area, R is the transmission range and A is the entire simulated area.

In [95], authors show the connectivity ratio with consistent views. When the buffer zone is 0 m and the average speed is about 1 m/sec, the connectivity ratio is very low as about 10%. However, when the buffer zone is set to 1 m, the connectivity ratio increases significantly. On the other hand, it is impossible to achieve 100% connectivity ratio under low mobility. Moderate and high mobility cause low connectivity

ratio. However, using consistent views achieve significant improvement on connectivity ratio. When using a buffer zone of 20 m in MANETs with an average speed of 10 m/sec, the connectivity ratio is about 40% without consistent views and 70% with consistent views. When using a buffer zone of 110 m and an average speed of 40 m/sec, the connectivity ratio reaches 98% with consistent views and 70% without consistent views.

The neighbors' list is the best method for a successful transmission and for broadcasting a frame to a subset of an updated neighbor list; it is used for route discovery to enhance packet delivery. Additionally, the network topology will remain effectively steady for appropriate time intervals. The update interval of neighbors' list is specified as a function of nodes' speed v. Moreover, the gossip scheme with flooding is used to determine and updates the list of neighbors. Because the network topology of MANETs changes significantly over time due to nodes' mobility, broadcasting is a fundamental communication primitive that can be used in route discovery in wireless ad hoc routing algorithms [96]. Flooding is a suitable approach in MANETs for broadcasting, as it requires no topological knowledge, where each node rebroadcasts the received frame to its neighbors upon receiving it for the first time.

4.5. The Mobility Model

Mobility and other various factors such as network size, routing scheme and traffic intensity may result in unpredictable variations in the overall network performance. However, nodes' mobility is a major factor that contributes to topology changes in ad-hoc networks. It has a dramatic effect on the performance of MANETs due to nodes mobility, which in return affects the whole performance of MANETs in terms

of routing protocol performance [40, 43], network throughput [97], location and resource management [98, 99, 100], topology control [101, 102, 103], system delay [36] and network connectivity [38, 104, 105]. However, The evaluation of network performance would be misleading and vary with time dramatically if a mobility model fails to provide a steady state speed [62].

The IEEE 802.11 RTS/CTS handshake mechanism is implemented under stationary and mobile network scenarios. The RWP mobility model is deployed in the mobile network scenario because of its simplicity and widely-used in many simulation studies of ad-hoc protocols [106]. The speeds of nodes are sampled from uniform and gamma distribution. This is to verify the performance of the IEEE 802.11 RTS/CTS under these two mobility patterns. We examine the system performance in terms of throughput, delay and retransmission rate for various numbers of nodes in the simulated area. In the case of stationary ad-hoc network scenario, 1-hop transmission is adopted. In the mobile scenarios, 1-hop routing and multi-hopping routing schemes are employed.

Chapter 5

FINITE QUEUEING MODEL OF IEEE 802.11 AD-HOC NETWORKS

In modeling ad-hoc networks, the assumption of infinite population is usually made. This is because finite queues are more difficult to analyze than the corresponding infinite queues [107]. However, such models lead to deficiencies in the model, since they do not hold in real applications. To ensure a realistic queuing model which describes the MAC protocol and nodes' behavior in the network environment more precisely. The IEEE 802.11 wireless networks of the RTS/CTS access mechanism is modeled under finite population assumption. The random access wireless ad-hoc networks is modeled as a closed-form *M/M/1/K/N* queueing networks.

Most traffic models consider infinite population for users where the nature of arrival process depends slightly on the number of users in the system only [108]. However, in real world applications, no such infinite populations exist. The finite population queue model has many applications in real world such as the number of cellular mobile subscribers, communication networks and statistical multiplexing. Finite buffer queues are difficult to analyze due to the necessity of minimizing the blocking probability by providing a sufficient buffer size. Blocking (loss) probabilities play an important role in the design and analysis of any queueing system. In such queues, if an arrival finds the buffer space full, it is blocked from entering into the system and considered lost.

There are some classical teletraffic methods used in the analysis of telecommunication systems with finite user population. The product-form queueing network models were introduced in [109] for open exponential networks and closed queueing network model with exponential servers were introduced in [110]. Markovian models with inter-arrival and service times are assumed to be exponentially distributed. It has been studied extensively with the development of telephone exchanges, and currently are utilized in data networks performance measurement evaluations [111]. The authors in [112] proposed a finite queueing model for evaluating the packet blocking probability and MAC queueing delays in a basic service set. In [113], an *M/MMGI/1/K* queueing model is developed for the analysis of IEEE 802.11 DCF using RTS/CTS over a single hop network. The IEEE 802.11 MAC based wireless ad-hoc network is modeled as a Markov modulated general arrival process. In [114], a discrete time *G/G/1* queueing model describes the behavior of the IEEE 802.11 non-saturation MAC layer and evaluates the queueing delays in finite load.

5.1. Finite Queueing System

Finite-source queueing models are systems in which there are a limited number of nodes which use the service offered by the system. Some of the known applications of this model are computer communication systems and machine-repairman problem. A simple example of finite population queueing system is the machine-repairman problem. A machine-repairman problem with N heterogeneous machines and C partially cross-trained repairmen (each repairman can repair only a subset of N machines, and that subset may or may not overlap with other repairmen's subsets of machines) has a wide application [115]. In this study, we consider a finite queueing system in which

the arrival packets are generated from a finite population with N identical nodes in a single transmission area and finite buffer of size K as showing in figure 5.1. The service time is exponential with mean value $1/\mu$, and arrival packet rate of each node is $\lambda_i = \Lambda/N$ arriving from an idle node and zero otherwise, where Λ is the total traffic load arrives each time slot.

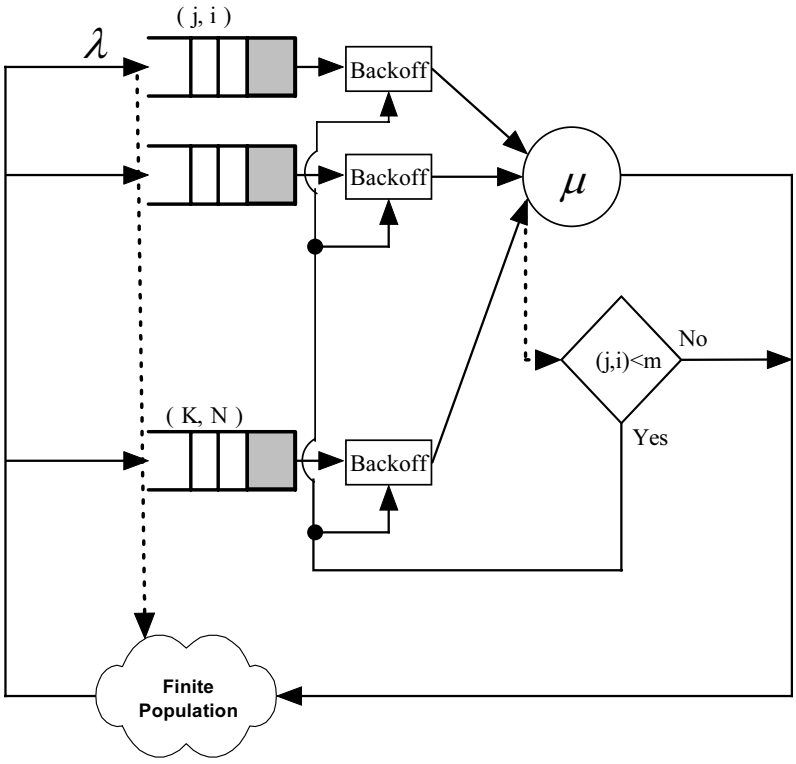

Figure 5.1. Wireless ad-hoc network queueing model.

The steady-state probabilities for finite-population queues are independent of the service distribution profile as long as the arrivals follow negative exponential distribution. Likewise, if the service time distribution is negative exponential, the system performance is invariant to the distribution of arrival times [116, 117]. The proposed queueing model of the *M/M/1/K/N* system can be expressed in Markov state transition as shown in figure 5.2.

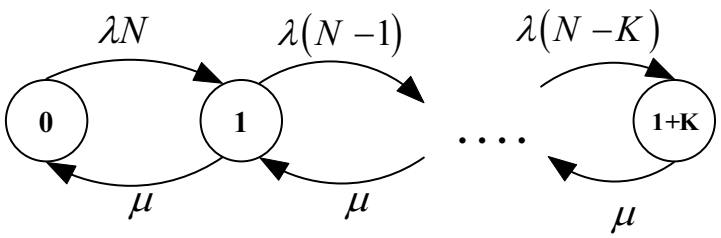

Figure 5.2. Markov chain state transition model of the *M/M/1/K/N* system.

The state probability of having i packets in the system, P_i is given by [118]:

$$P_i = \begin{cases} P_0, & i = 0 \\ \frac{N!}{(N-i)!}\left(\frac{\lambda}{\mu}\right)^i P_0, & i = 1, 2, ..., N+1 \end{cases}$$

$$P_0 = \left[1 + \sum_{i=1}^{N} \frac{N!}{(N-i)!}\left(\frac{\lambda}{\mu}\right)^i\right]^{-1}. \tag{5.1}$$

By means of little's law [119], the mean packet delay in the system W is given by

$$W = \frac{L}{\lambda_e}. \tag{5.2}$$

The average number of packets of each node in the system L are given by

$$L = \sum_{i=1}^{K+1} iP_i, \tag{5.3}$$

λ_e represents the long run effective arrival rate of packets to the queue and is computed

as follow:

$$\begin{aligned}\lambda_e &= \sum_{i=1}^{K+1} \lambda_i P_i = \sum_{i=1}^{K+1} \lambda(N-i)P_i \\ &= \lambda \left[\sum_{i=1}^{K+1} NP_i - L \right]. \end{aligned} \tag{5.4}$$

5.1.1. Blocked Customers Delayed System

Figure 5.3 shows the blocked customers delayed (BCD) system. N is the number of identical independent nodes of the population and K is the buffer queue size of each node. In such a system, packet arrival rates change with the state of the system. This may depend on N (population size) and $\lambda_i's$ (packet arrival rates). Therefore, ignoring packet arrival rates and applying the $C\mu$ rule is not always optimal in a finite-population queueing system as investigated in [120]. This observation motivates us to study the effect of finite-population systems with packet arrival rates on CSMA/CA in order to find the optimal independent of packet arrival rate, population size, and number of packets in the system.

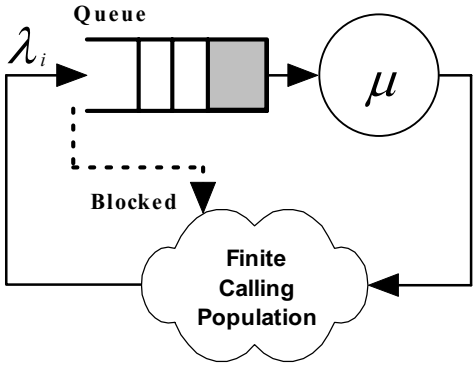

Figure 5.3. BCD queueing system.

Once a node seizes the medium, it starts sending its packets to the intended destination

and blocks other nodes requests from accessing the medium for a period of time $t = T_{RTS}+T_{CTS}+T_D+T_{ACK}+3SIFS+4\tau$. However, every request for a service affects the system state and a busy node becomes idle at a rate of μ. Therefore, the death rate μ_i is given by [118]:

$$\mu_i = \begin{cases} 0, & i = 0 \\ \mu, & i = 1, 2, ..., N. \end{cases} \tag{5.5}$$

The birth rate λ_i is given by

$$\lambda_i = \begin{cases} \lambda\left(N - i\right), & 0 \leq i \leq K \\ 0, & i > K. \end{cases} \tag{5.6}$$

The average queue length of each node in the first stage L_q, is given as follows

$$L_q = \sum_{i=2}^{K+1}(i-1)P_i. \tag{5.7}$$

The average waiting queue time of packets in the first stage is the ratio of L_q and the long run effective arrival rate of packets λ_e, W_q is given by:

$$W_q = \frac{L_q}{\lambda_e}. \tag{5.8}$$

Blocking probability $P_{B(BCD)}$ in BCD system is the probability that the node finds the buffer queue full when placing a packet for transmission. This is the probability that

the packet must return to the finite population.

$$\begin{aligned} P_{B(BCD)} &= P_{1+K} \\ &= \frac{N!}{(N-K-1)!}\left(\frac{\lambda}{\mu}\right)^{K+1} P_0. \end{aligned} \tag{5.9}$$

As with the finite population models, it is often useful to think in term of offered load ρ_o. Offered Load is defined as the total traffic load (new arrival and retransmitted packets) submitted to the network. In BCD, ρ_o is given by

$$\rho_o = \frac{\rho}{1-\rho} = \frac{\lambda}{\mu - \lambda}, \tag{5.10}$$

where $\rho = \lambda/\mu$ is the offered load/idle node.

5.1.2. Blocked Customers Cleared System

Blocked customers cleared (BCC) system is shown in figure 5.4. It is a finite queueing system without an input buffer queue. Each node independently generates a packet at rate λ_i when idle and zero otherwise. Since blocked nodes are assumed cleared, a new request will affect the state if and only if there is at least one channel is idle. In our model, one serving channel is used only. Hence, we have the birth rate as follows

$$\lambda_i = \begin{cases} \lambda N, & i = 0 \\ 0, & \text{Otherwise.} \end{cases} \tag{5.11}$$

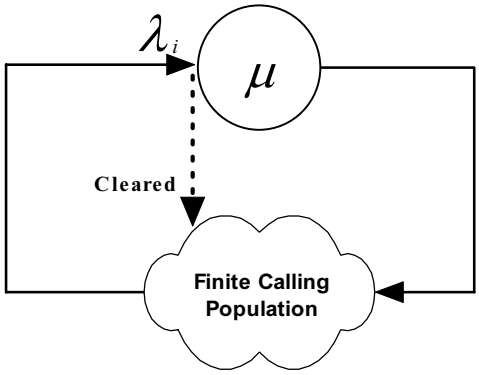

Figure 5.4. BCC queueing system.

The long run effective arrival rate of packets to the server is given by:

$$\lambda_e = \rho_o \, \mu = \mu. \tag{5.12}$$

The mean packet delay of the second stage W is given by

$$W = \frac{L}{\lambda_e} = \frac{1}{\mu}. \tag{5.13}$$

Engset formula for determining the probability that a packet is lost or clear in BCC system stage $P_{clr(BCC)}$, it is the probability that the node finds the medium busy [121]. Clear packets are returned to calling population provided that the backoff stage m reaches its maximum.

$$\begin{aligned} P_{clr(BCC)} &= P_1 \\ &= \frac{N!}{(N-1)!} \left(\frac{\lambda}{\mu}\right) P_0. \end{aligned} \tag{5.14}$$

When blocked packets are cleared, the offered load is lower bounded by the intended offered load. In accordance with the general Engset formula, the state probabilities in the finite population BCC systems with non-identical packets depend only on the mean service times and mean idle-packet interarrival times for each packet.

The two stages queue of figure 5.1 are statistical independent. Therefore, the total blocking probability P_B is computed from (5.9) and (5.14) as follows

$$\begin{aligned} P_B &= P_{B(BCD)} + P_{clr(BCC)} \\ &= P_{1+K} + P_1 \\ &= N!\, P_0 \frac{\lambda}{\mu} \left[\frac{1}{(N-K-1)!} \left(\frac{\lambda}{\mu}\right)^K + \frac{1}{(N-1)!} \right]. \end{aligned} \tag{5.15}$$

The throughput S of the system is given in terms of blocking probability P_B and long run effective arrival rate as follows

$$S = \lambda_e\,(1 - P_B). \tag{5.16}$$

The total mean packet delay of the system $\bar{D}$ is computed from (5.8) and (5.13) as follows

$$\bar{D} = N\,W_q + W + B_o, \tag{5.17}$$

where B_o is the backoff time of the BEB algorithm as explained in chapter 4.

Chapter 6

SIMULATION RESULTS

6.1. Introduction

This chapter provides simulation results to validate the performance evaluation of mobility models, effect of mobility on CSMA/CA scheme and finite queueing network of CSMA/CA protocol. All simulations are carried out using the MATLAB Software Package.

6.2. RWP mobility models

In the given RWP mobility models, each node chooses an initial location and destination point independently from a random uniform distribution. 50 nodes are assumed to be uniformly distributed and moving independently in a square region with a size of 1000m $\times$ 1000m simulation area. The speed is chosen randomly in the interval of $[V_{min}, V_{max}]$ and sampled from the designated distribution. The clipped normal distribution parameters; $\mu = \frac{1}{2}(V_{max} + V_{min})$ and $\sigma = \frac{1}{4}(V_{max} - V_{min})$, the Gamma distribution parameters; $\alpha = \frac{1}{2}(V_{max} + V_{min})$ and $\beta = 1$. Simulation results are obtained by averaging 30 distinct scenarios over 3000 seconds with a 98% confidence interval. Pause time is set to zero to indicate continuous mobility unless pausing is indicated. Pause time is chosen independently from a random uniform distribution in the interval of 0 - 60 seconds.

6.2.1. Instantaneous Average Node Speed

Figure 6.1 shows the performance of various RWP mobility models. The average speed in the traditional RWP model; $U \sim [0, 20]$ drops about 50% from the expected 10 m/sec within the first 250 seconds. Also, it continues in decreasing below the level of 4 m/sec; this model may not reach the steady state. While the modified RWP model; $U \sim [1, 19]$ proposed in [31], the average node speed converges to the steady state after 250 seconds and stabilizes at an average speed value of 6 m/sec. For the model proposed in [62], where node's speed is sampled from clipped normal distribution; $N \sim [V_{max}, V_{min}]$. The clipped normal distribution model; $N \sim [1, 19]$ could achieve a maximum average node speed of about 7.7 m/sec. While the model proposed in [63], node's speed is sampled from Beta(2,2) distribution; $\beta \sim [V_{max}, V_{min}]$. This model could achieve a maximum instantaneous average node speed of about 6.67 m/sec at $\beta \sim [0, 20]$ and about 7.84 m/sec at $\beta \sim [1, 19]$. However, in the proposed GRWP model, node's speed is sampled from Gamma distribution; $\Gamma \sim [V_{max}, V_{min}]$. In the given model; $\Gamma \sim [1, 19]$, the steady state is achieved faster than the other existing models and the average speed stabilizes approximately at 8.98 m/sec. Additionally, the instantaneous average node speed does not decay to zero as $V_{min} \longrightarrow 0$ and achieves faster convergence to the steady state as well as in the $\Gamma \sim [1, 19]$ scenario. It is clear that GRWP model outperforms the mentioned RWP models and provides a significant performance improvement in terms of having a higher steady state speed and achieving faster convergence to the steady state.

Figure 6.2 shows the instantaneous average node speed of various speed distributions of RWP mobility models at a network size of N = 100 and 200 nodes. The results

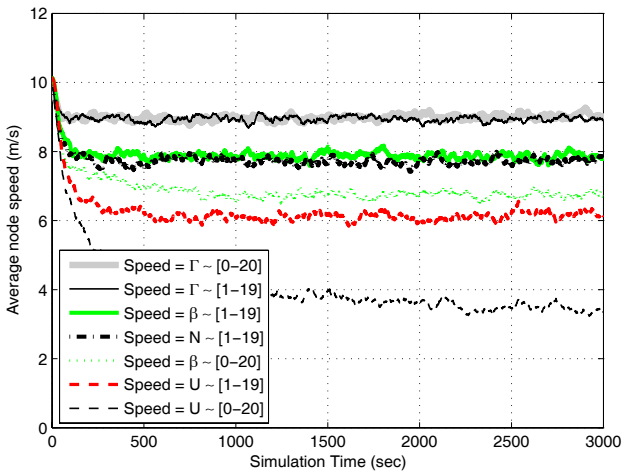

Figure 6.1. Instantaneous average node speed of various speed distributions of RWP mobility models at network size N = 50 nodes.

for all given speed distributions of the RWP mobility models show that, as the number of nodes increase, the fluctuation of the average node speed is reduced. However, the network size has little effect on the average speed values.

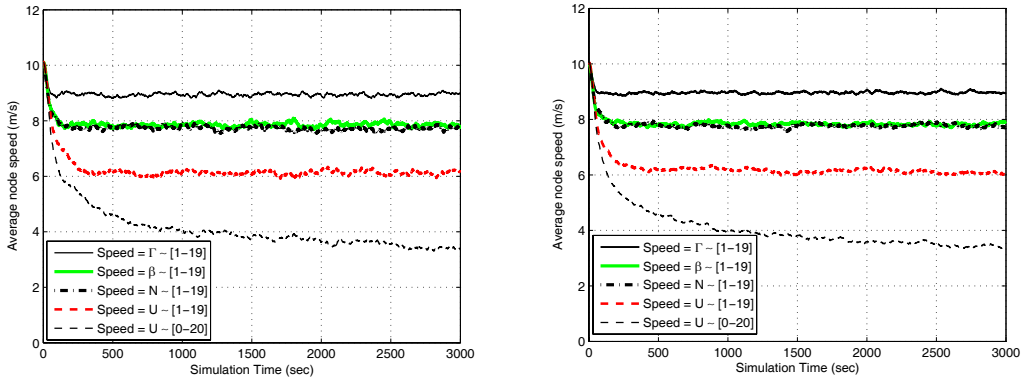

(a) N = 100 nodes (b) N = 200 nodes

Figure 6.2. Instantaneous average node speed of various speed distributions of RWP mobility models at various network size.

The analytical and simulation results of various scenarios of the proposed GRWP model are presented in figure 6.3. In mobile scenario, the figure shows that the av-

erage nodes speed of the analytical and simulation curves match very well. Similarly, in pausing scenario, both the analytical and simulation model results are similar. Table 6.1 illustrates various speed ranges of the proposed GRWP model without pausing. $E[\bar{V}]_{initial}$ is the pre-assumed average speeds and defined as $\frac{1}{2}(V_{max}+V_{min})$. The analytical and simulation results indicate that the proposed GRWP model provides average values closer to the pre-assumed average speeds.

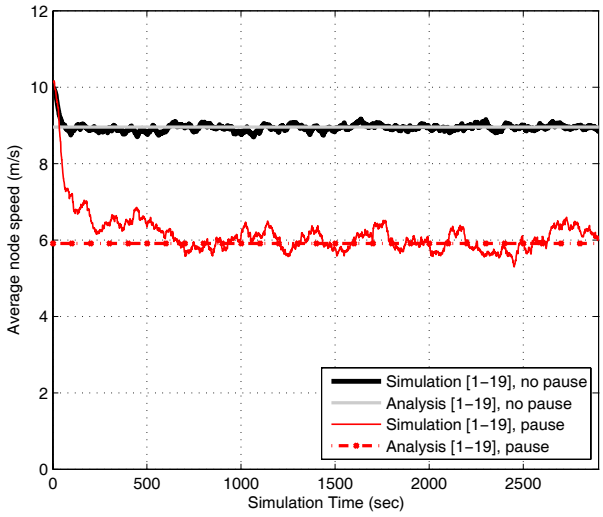

Figure 6.3. Instantaneous average node speed of the proposed GRWP mobility model.

6.2.2. Density of Nodes' Speed

Figure 6.4 shows the pdf of nodes' speed for the traditional RWP mobility model $(U \sim [0, 20])$ at different time instants. The figure presents the histogram for the density of nodes' speed at the first, 100^{th} and 3000^{th} seconds of movement. As shown in figure 6.4(a), the density of nodes' speed at the first second of movement is close to uniform distribution with a mean of 9.72 m/sec and a variance of 36.9. Figure 6.4(b), shows the density of nodes' speed after 100 seconds of movement. A rapid change in

Table 6.1. Various speed ranges of the proposed GRWP mobility models (m/sec) without pausing.

Speed range	$E[\bar{V}]_{initial}$	$E[\bar{V}]_{analysis}$	$E[\bar{V}]_{simulation}$
$[0.5, 1.0]$	0.75	0.69	0.70
$[0.5, 1.5]$	1.00	0.83	0.84
$[1.0, 2.0]$	1.50	1.39	1.40
$[1.0, 3.0]$	2.00	1.68	1.70
$[1.0, 4.0]$	2.50	1.97	1.99
$[1.0, 5.0]$	3.00	2.28	2.31
$[1.0, 6.0]$	3.50	2.63	2.65
$[1.0, 7.0]$	4.00	3.03	3.06
$[1.0, 19.0]$	10.0	8.95	8.98
$[0.0, 20.0]$	10.0	8.94	8.96

the distribution of nodes' speed is observed and the density of nodes' speed is concentrated below 9 m/sec. The nodes' speed has a mean value of 6.77 m/sec and a variance of 33.59. The distribution of nodes' speed after 3000 seconds of movement is shown in Figure 6.4(c). The density of nodes' speed is concentrated heavily below 3 m/sec with a mean of 3.13 m/sec and a variance of 23.81. The figure illustrates that the traditional RWP mobility model ($U \sim [0, 20]$) is insufficient in modeling the speed distribution of the nodes since the distribution deviates from the initial uniform distribution.

The density of nodes' speed for the modified RWP mobility model ($U \sim [1, 19]$) is shown in figure 6.5. The figure depicts the histogram for the density of nodes' speed at the 100^{th} and the 3000^{th} seconds of movement. As shown in figure 6.5(a), the

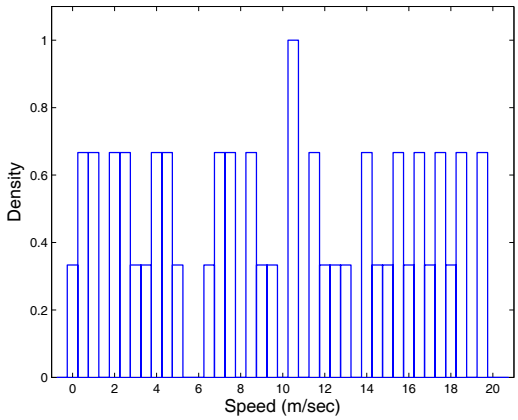

(a) Speed at the first one second of movement

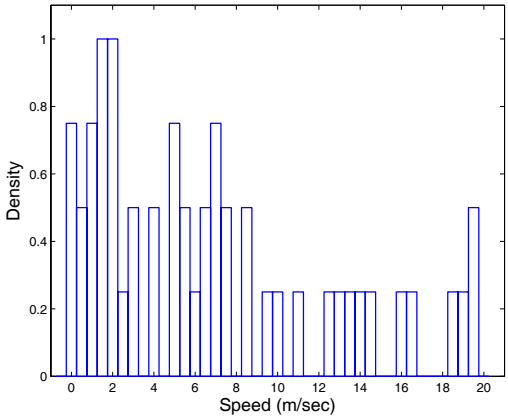

(b) Speed at the 100 seconds of movement

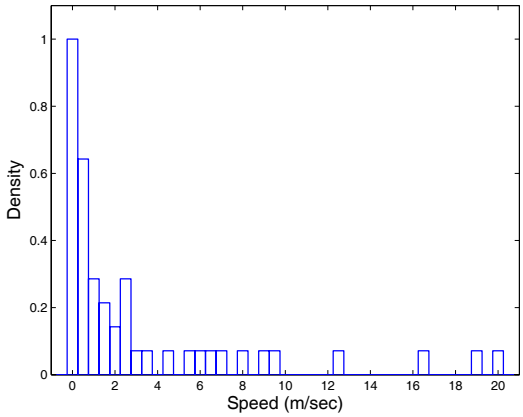

(c) Speed at the 3000 seconds of movement

Figure 6.4. The node speed density of the typical RWP model ($U \sim [0, 20]$).

density of nodes' speed after 100 seconds has a distribution different from the initial distribution. The nodes' speed density spreads between 1 - 19 m/sec with a mean value of 6.88 m/sec and a variance of 28.03. Figure 6.5(b) shows the histogram for the density of nodes' speed after 3000 seconds of movement. The nodes' speed density is spread between 1 - 18 m/sec and is concentrated below 6 m/sec with a mean value of 5.98 m/sec and a variance of 20.28. It is clearly seen in figure 6.4(c) and 6.5(b) that the modified RWP mobility model ($U \sim [1, 19]$) outperforms the traditional RWP mobility model ($U \sim [0, 20]$). In the traditional RWP model, the probability of finding

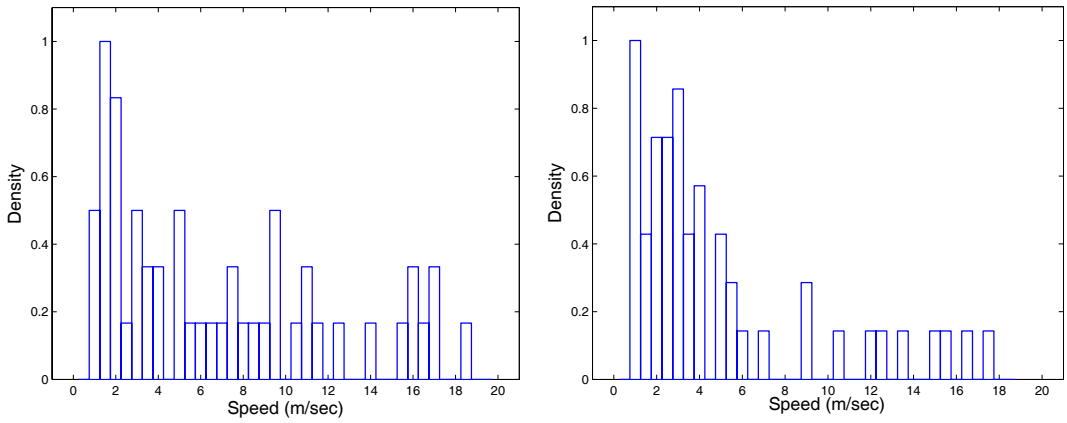

(a) Speed at the 100 seconds of movement (b) Speed at the 3000 seconds of movement

Figure 6.5. The node speed density of the modified RWP model ($U \sim [1, 19]$).

nodes' speed above 5 m/sec is about 0.22 and the normalized density is about 0.1. While in the modified RWP model, the probability of finding nodes' speed above 5 m/sec is about 0.32 and the normalized density is about 0.2.

Figure 6.6 shows the speed of nodes for the proposed GRWP model ($\Gamma \sim [1, 19]$). The figure presents the histogram for the density of nodes' speed at the first, 100^{th} and 3000^{th} seconds of movement. As shown in figure 6.6(a), the density of nodes' speed at the first second of movement is close to the initial speed distribution of nodes, which are sampled from Gamma distribution. The nodes' speed density is spread between 6.5 - 15.7 m/sec with a mean of 10.07 m/sec and a variance of 4.16. Figure 6.6(b) shows the histogram for the density of nodes' speed after 100 seconds of movement. The nodes' speed density is spread between 6.8 - 14 m/sec with a mean value of 9.7 m/sec and a variance of 2.57. The average speed is 3.6% lower than the average speed at the first second of movement. Furthermore, the node speed distribution at the 100 seconds of movement is similar to the corresponding distribution at the initial state.

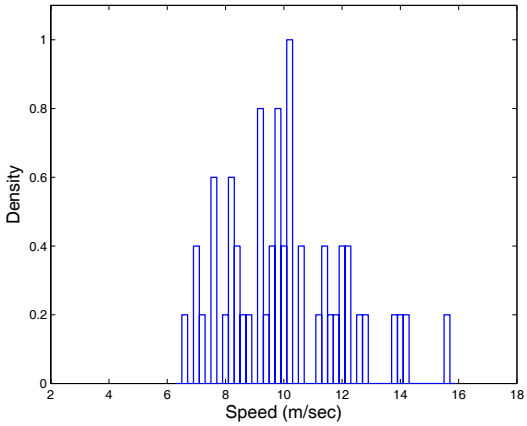

(a) Speed at the first one second of movement

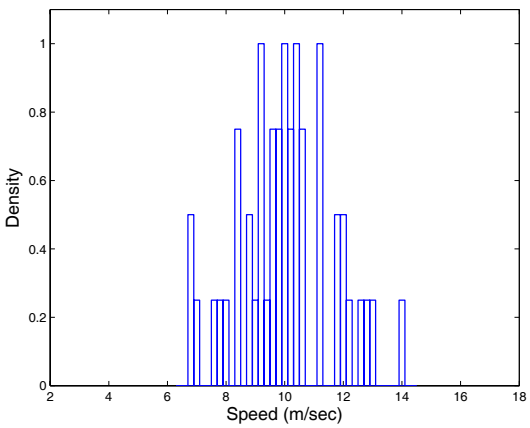

(b) Speed at the 100 seconds of movement

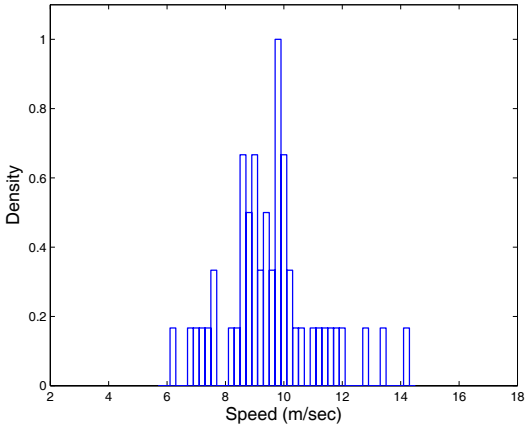

(c) Speed at the 3000 seconds of movement

Figure 6.6. The node speed density of the proposed GRWP model ($\Gamma \sim [1, 19]$).

Additionally, the convergence to the steady state is fast. The histogram for the nodes' speed density after 3000 seconds of movement is shown in figure 6.6(c). The node speed distribution at any time instant of the simulation (e.g., at 3000 seconds of movement) is similar to the corresponding distribution at the initial state. Also, it is shown that the speed distribution of nodes is close to Gamma distribution and the density of speed is spread between 6.2 - 14.2 m/sec. Moreover, the density of nodes' speed is concentrated around the mean of 8.98 m/sec and has a variance of 2.6.

6.3. The Effect of RWP Mobility on CSMA/CA Performance

The results for the RWP mobility model are obtained by taking the average of 30 distinct scenarios of the simulated time. Also the figures of CSMA/CA scheme are obtained by generating 10 sample runs for each data point. This is to have accurate results. Each node chooses an initial location and destination point independently from a random uniform distribution, where nodes are uniformly distributed and move independently in a square region of 1000m $\times$ 1000m simulation area. The speed is chosen randomly in the interval of $[V_{min}, V_{max}]$ and sampled from the designated distribution. The initial data observed at the first 500 sec in the RWP mobility model $(U \sim [1, 19])$ are disregarded in simulating the CSMA/CA scheme, as well the first 100 sec in the GRWP mobility model $(\Gamma \sim [1, 19])$. This is to insure that the system enter the steady state. Pause time is set to zero to keep continues mobility. The GRWP mobility model proposed in [**?**, 46] outperforms the modified RWP [31] mobility models. It provides a significant performance improvement in terms of having a higher steady state speed and achieving faster convergence to the steady state. The average speed in the modified $(U \sim [1, 19])$ and GRWP mobility models $(\Gamma \sim [1, 19])$ are about 6 m/sec and 8.98 m/sec, respectively.

In the CSMA/CA scheme, a node generates a request at an arrival rate λ = 100 packets/sec to access the medium. The node transmits a unicast or a broadcast frame using the RTS/CTS (4-way handshake). The traffic is assumed to spread across the network if the destination node is out of range with the source node, this is in accordance with the ad-hoc network scenarios. Furthermore, the traffic spreads to as many relay nodes as possible, and delivered to the destination node as soon as any of the relaying nodes

is in range with the destination node. Each node generates 512 byte of data packet size and transmits at a constant bit rate (CBR) of 11 Mbps to a random chosen destination node. During simulation, nodes' movement is updated every 4 sec in accordance to the designated mobility models. Other parameters are listed in table 6.2.

Table 6.2. Validation parameters used

Basic bit rate (BBR)	1Mb/s	PHY header	192 bits
MAC header	272 bits	RTS	160 bits
CTS	112 bits	ACK	112 bits
SIFS	$10\mu s$	DIFS	$50\mu s$
Slot Time (δ)	$20\mu s$	CWmin	32
Backoff stage (m)	5	Propagation Delay(τ)	$1\mu s$
Simulated Time	100 sec		

Figure 6.7 shows the average throughput of the RTS/CTS mechanism of variable number of nodes in the network. The minimum throughput is 0.24 and 0.027 at a network size of 5 nodes for the stationary and mobile network scenarios with multi-hopping routing scheme, respectively. The maximum throughput of about 0.7 is obtained at a network size of 20 nodes, this is for the stationary and mobile network scenarios with multi-hopping routing scheme. However, the mobile network scenarios with 1-hop route can achieve at most a maximum throughput of 0.038 at a network size of 50 nodes. Also, the results show that under mobility, the multi-hopping routing scheme can take advantage of nodes' movement to achieve higher path availability and end-to-end throughput compared to the 1-hop routing scheme.

Figure 6.8 shows the average delay of the RTS/CTS mechanism of variable number

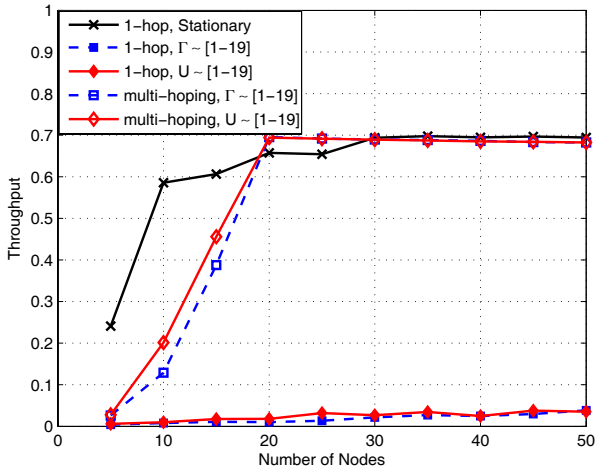

Figure 6.7. Average throughput of the RTS/CTS mechanism.

of nodes in the network. As the number of nodes increases, the average delay keeps in increasing, especially in the case of mobile network scenarios with multi-hopping routing scheme. Although the Gamma RWP model has a higher average speed compared to the uniform RWP model, the average delay induced by both RWP mobility patterns in the mobile network scenario is similar. The maximum average delay is almost 17 sec and 145 sec at a network size of 50 nodes for the stationary and mobile network scenarios with multi-hopping routing scheme, respectively. While the maximum average delay of the mobile network scenario with 1-hop route is about 5 sec at a network size of 50 nodes. Mobile network scenario with multi-hopping routing scheme involves large delays, this is because of packet routing and buffers.

Figure 6.9 shows the packet retransmission rate of the RTS/CTS mechanism of variable number of nodes in the network. As the number of nodes increases, the packet retransmission rate increases up to a maximum value of 48 and 139 at a network size of 50 nodes. This is for the stationary and the mobile network scenarios with multi-

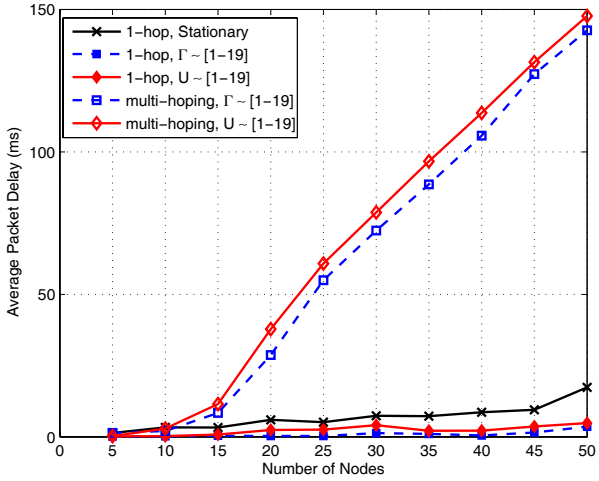

Figure 6.8. Average system delay of the RTS/CTS mechanism.

hopping routing scheme, respectively. While the packet retransmission rate for the mobile networks scenario with 1-hop route is too small. This is because the time fraction of two nodes to be in range is too small, thus most of nodes are out of range most of the time and cannot access the medium. Also, it should be noted that the failure of packet delivery and/or packet collision, in turn increases the packet retransmission rate.

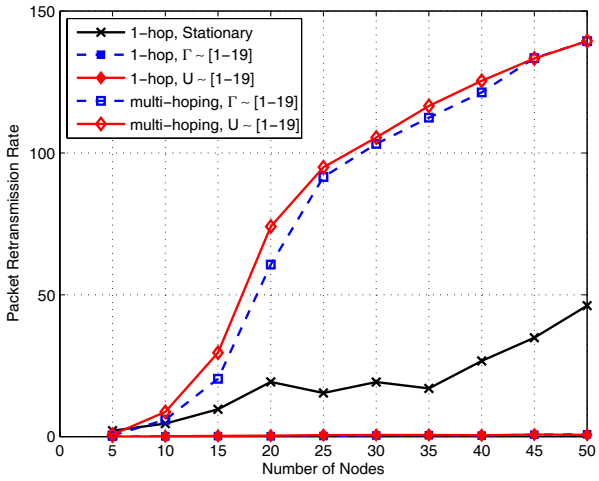

Figure 6.9. Packet retransmission rate of the RTS/CTS mechanism.

The average number of sub-network and network connectivity of all nodes are investigated from a global network point of view, where a node can reaches any other nodes via multi-hop path. The simulation results of stationary and mobile node scenarios in figure 6.10 are drawn at a constant transmission range of R = 250m. In mobile node scenario, nodes move with respect to RWP mobility model ($U \sim [1, 19]$), where nodes take advantage of their mobility to compensate the low network connectivity. In both scenarios, the average number of sub-network decreases as the number of nodes increases and the results of both scenarios' behavior are similar. While the probability of network connectivity $P(\mathrm{con})$ increases as the number of nodes increases. When the threshold node size is reached, the network is fully connected. Furthermore, the desired probability of $P(\mathrm{con})$ = 100% of the stationary and mobile node scenarios are obtained at N = 60 and 50 nodes, respectively.

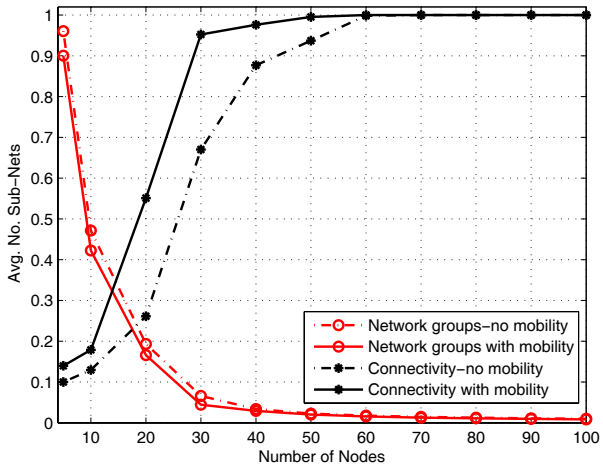

Figure 6.10. Increasing the network size at transmission range of R = 250m.

Figure 6.11 shows the simulation results for the average number of sub-network and the $P(\mathrm{con})$ over the transmission range R at a network size N = 50 nodes. At low transmission range, the network connectivity remains zero until a certain threshold

range is reached. Once the transmission range is larger than this threshold, the $P(\mathrm{con})$ increases until the network is almost surely connected. For example, in stationary and mobile node scenarios, the network is almost a disconnected network until a threshold range R = 125m and 25m, respectively. Meanwhile, the network is connected with probability $P(\mathrm{con}) = 94\%$ at transmission range of R = 250m and 170m, respectively. However, in stationary node scenario, the desired probability $P(\mathrm{con}) = 100\%$ can be achieved at R = 275m. In mobile node scenario, the desired probability $P(\mathrm{con}) = 100\%$ can be achieved at R = 250m. The average number of sub-network in stationary and mobile node scenarios is about 0.12 and 0.02 at R = 150m, respectively. Hence, at low transmission range the average number of sub-network is large and the network connectivity is obviously lost. On the other hand, a very high transmission range causes interference among nodes in the network. The range should be large enough to keep the network connected, but it should still be small enough to avoid the low interference between nodes. Clearly, very small values of R and N create networks that are disconnected.

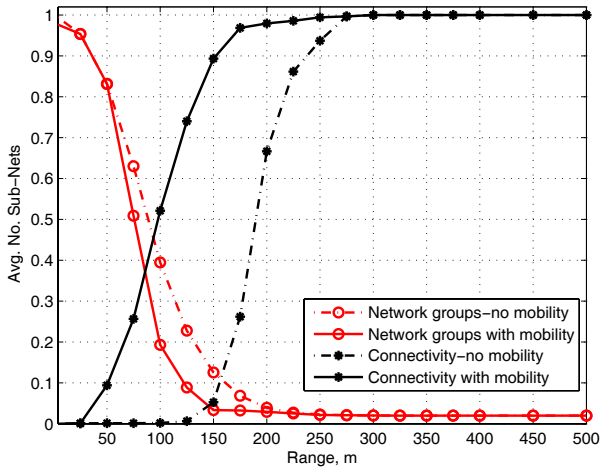

Figure 6.11. Increasing the transmission range at network size N = 50 nodes.

6.4. Queueing Network Model

In simulating the finite queueing model *M/M/1/K/N* of the CSMA/CA scheme. A stationary 1-hop network is assumed, where each node generates a request at an arrival rate $\lambda = [0.1 - 100]$ to access the medium and the queueing discipline of all nodes are assumed to be first come first served (FCFS) queueing discipline. The node transmits unicast frames using the RTS/CTS access mechanism (4-way handshake). Each node transmits at a constant bit rate (CBR) of 11 Mbps to the destination node.

Figure 6.12 illustrates the queueing system flow chart of the IEEE 802.11 DCF. A node seizes the medium if idle, then the node sends its packets to the intended destination and blocks other nodes requests from accessing the medium for the period of transmission time. However, if the medium is busy, the generated packet is cleared and returns back to the calling population and starts thinking (long-run effective arrival time of packets) provided that the packet reaches its maximum backoff stage m.

6.4.1. Packet Arrival Rates

Figure 6.13 shows the effective throughput for different arrival rates at population sizes of N = 20 and 50 and packet sizes of 512 and 1024 bytes. As the arrival rate increases (increasing number of packets in the system), effective throughput increases until it reaches the maximum throughput of 0.8. At a certain arrival rate, the effective throughput remains steady for both population sizes of N = 20 and 50. This occurs because as the arrival rate increases, the utilization increases, which in turn force the arrival rate to step down in order to regulate the system (forcing the system to remain in the steady state). This implies that IEEE 802.11 RTS/CTS handshake and finite population

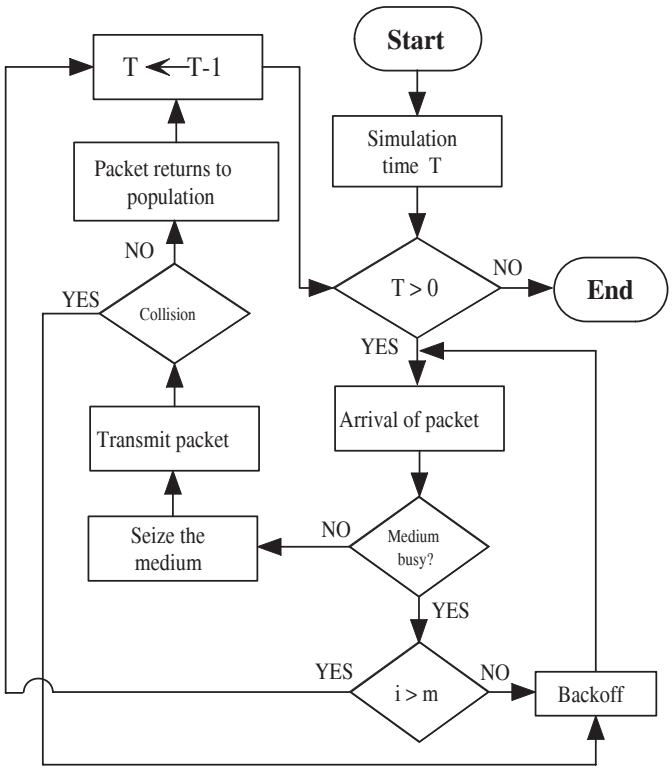

Figure 6.12. Simulation flow chart of finite queueing model for CSMA/CA scheme.

models are self-regulatory. Regardless of the population size, arrival rate with packet size 1024 bytes has a higher effective throughput than for the packet size of 512 bytes, while larger population sizes reach the maximum effective throughput at a lower arrival rate compared to the smaller population sizes. This is because probability of packet arrival depends directly on the number of idle nodes in the system that is available to generate new requests for transmission. Therefore, more requests are being generated at a low arrival rate in the case of high population sizes.

The results of average packet delay for different packet and population sizes are considered as shown in figure 6.14. Packet delay at low arrival rate is small and similar for all scenarios up to almost of $\lambda = 1$ packets/sec. While at larger arrival rates greater than

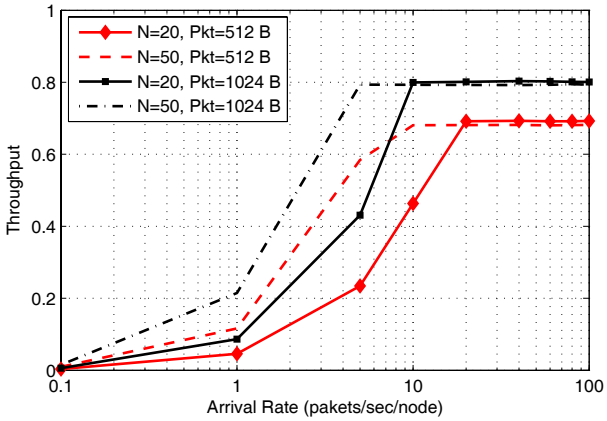

Figure 6.13. Arrival rate vs effective throughput.

$\lambda = 1$ packets/sec, large packet and population sizes has a larger packet delay compared to small packet and population sizes, this is because large packets seize the medium longer than small packet sizes, thus push more packets upon arrival into backoff stage. As the arrival rate increases, average packet delay increases up to its maximum. However, large packet sizes start failing at an arrival rate of $\lambda = 60$ packets/sec. This is because nodes reach the threshold point and shut off the stream of requests for a regulatory purpose. Regardless of packet size, average delay of large population size is higher compared to small population sizes. This is due to more blocked packets are being delayed in the backoff. When maximum backoff stage is reached, packets in the backoff state are cleared and return to the calling population, which in turn increase the arrival rate.

6.4.2. Buffer Thresholds

Figure 6.15 shows the effect of variable buffer thresholds on networks' throughput at a population size of $N = 50$ nodes. At a buffer threshold capacity of 0.01, the effective throughput of packet size of 512 bytes increases rapidly and reaches a throughput

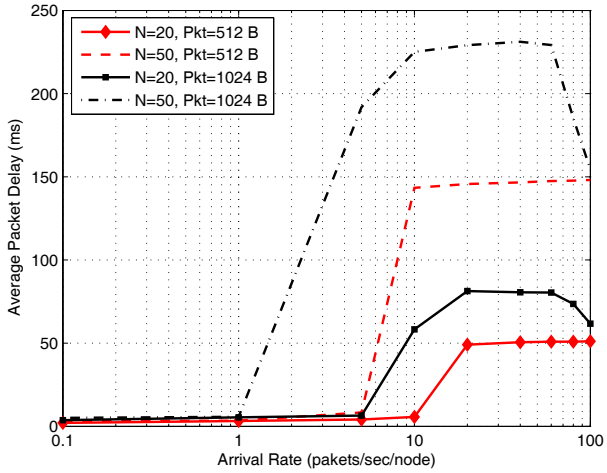

Figure 6.14. Arrival rate vs average packet delay.

of 0.5, meanwhile the throughput of packet size of 1024 bytes increases gradually. Approximately at a buffer threshold of 8 Mb, the steady state throughput of both packet sizes of 512 and 1024 bytes are 0.7 and 0.8, respectively. Therefore, for a maximum throughput, the minimum selected buffer threshold should be at least 8 Mb.

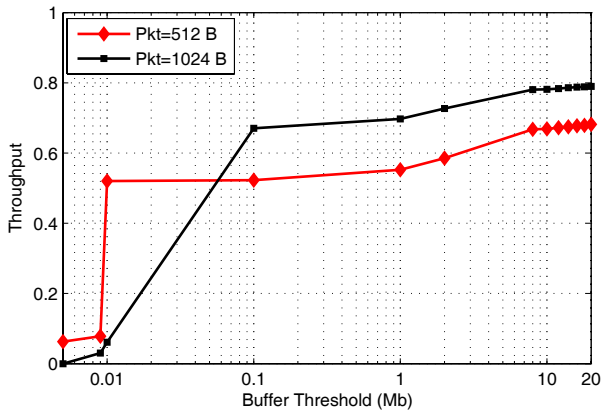

Figure 6.15. Buffer threshold vs effective throughput at $N = 50$.

As shown in figure 6.16, packet delay is obtained at variable buffer thresholds and at population size of $N = 50$ nodes. Packet delays of both packet sizes increase exponen-

tially as the buffer threshold increases. However, packet delays of both packet sizes are similar especially at small buffer threshold below 2 Mb. However, at a buffer threshold of 20 Mb, the maximum packet delay of packet sizes 512 and 1024 bytes are 145 and 175 msec, respectively.

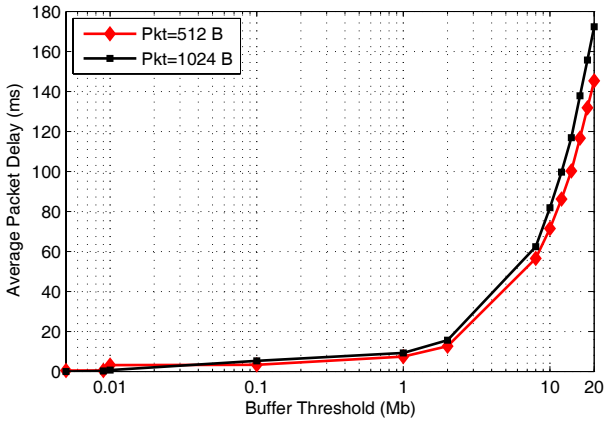

Figure 6.16. Buffer threshold vs average packet delay at $N = 50$.

Chapter 7

CONCLUSIONS AND FUTURE WORK

7.1. Conclusions

MANETs employ a common shared medium in order to facilitate communications among nodes in the network. A collision occurs at the receiving nodes if there are more than one node transmits frames at the same time. The collided frames are lost as well the medium bandwidth is wasted during the collision period. Therefore, an efficient medium access protocol is needed to regulate the sharing of common resources fairly among distributed nodes, minimize collisions between nodes and provide a better connectivity environment. In the IEEE 802.11 for CSMA/CA based RTS/CTS mechanism, the collided packets are usually RTS control packets.

The existing RWP mobility model suffers from speed decay as the simulation progresses and may not reaches the steady state. Also, the probability distributions of nodes' speeds vary continuously over the simulation time. GRWP mobility model is proposed to overcome these problems, where speed of nodes are sampled from Gamma distribution for more precise distribution and better modeling of the nodes' speed. The proposed GRWP mobility model is motivated by the need for speed distribution that preserves the initial nodes' speed distribution over simulation time. The analysis and simulation results indicate that the proposed GRWP mobility model outperforms the

existing RWP mobility models and provides a significant performance improvement in terms of having a higher steady state speed and fast convergence to the steady state. The proposed model provides an average speed value close to the desired average speed than those of the existing RWP mobility models. Moreover, the probability distribution of nodes' speed is steady over the simulation time.

Also, the throughput performance improvement can be obtained through the exploitation of nodes' mobility and multi-hopping routing. The simulation results of the mobile network scenario show that mobility leads to a throughput enhancement and a higher path availability for the multi-hopping routing scheme. The collected result of the mobile ad-hoc network scenario with multi-hopping routing scheme, implies that the average throughput remains constant and there is no loss in the throughput as the number of nodes per unit area increases. However, the disadvantage of this scenario is that it involves large delays. This is in tradeoff with the end-to-end effective throughput.

In modeling the IEEE 802.11 DCF as a closed-form queueing network and with the assumption of finite population. The proposed model ensures more realistic queueing model since it describes the MAC protocol and nodes' behavior in the network environment more precisely. Simulation results show that larger packet sizes result in higher effective throughput and larger population sizes result in higher average delay especially at high arrival rates. It is also shown that as the buffer threshold increases, the average delay increases exponentially. A distinguishable remark of finite queueing model and IEEE 802.11 DCF is that both are self-regulatory. This is because the stream of requests shuts off completely when there are no idle nodes available in the

system.

7.2. Future Work

The main objective of MAC protocol is to access the shared limited bandwidth medium efficiently. Therefore, An efficient medium access protocol is needed to overcome the limited bandwidth in wireless ad-hoc network for better performance enhancement and high network throughput. Future work may include the use of robust header compression (ROHC) technique over the CSMA/CA based RTS/CTS handshake mechanism for efficient utilization.

The propose GRWP mobility model outperforms the existing RWP mobility models in terms of having a higher steady state speed, achieving faster convergence to the steady state and the advantage of probability distribution of nodes' speed remaining steady over the simulation time. Future research may include the study of other probability distributions of nodes' speed and their effects on ad-hoc network protocols.

REFERENCES

[1] IEEE computer society LAN MAN standards committee, "Wireless LAN medium access protocol (MAC) and physical layer specification", *IEEE Std 802.11 1997, Institute of Electrical and Electronic Engineers*, NY, March 1999.

[2] J. Weinmiller, M. Schlager, A. Festag and A. Wolisz, "Performance study of access control in wireless LANs IEEE 802.11 DFWMAC and ETSI RES 10 HIPERLAN", *Mobile Networks and Applications*, vol. 2, pp. 55-67, 1997.

[3] Z. J. Haas, J. Deng and S. Tabrizi, "Collision-free medium access control scheme for ad-hoc networks", *In Proceedings of the IEEE Military Communications Conference (MILCOM' 99)*, vol. 1, pp. 276-80, 1999.

[4] IEEE 802.11 wireless local area networks - The working group for WLAN standards, "ANSI/IEEE Std 802.11, part 11: Wireless LAN medium access control (MAC) and physical layer (PHY) specifications", *Tech. rep., IEEE 802 LAN/MAN Standards Committee*, 1999.

[5] T. You, C. H. Yeh and H. S. Hassanein, "DRCE: A high throughput QoS MAC protocol for wireless ad-hoc networks", *In Proceedings of the IEEE International Symposium on Computer Communications (ISCC' 05)*, pp. 671-676, 2005.

[6] C. L. Fullmer and J. J. Garcia-Luna-Aceves, "Solutions to hidden terminal problems in wireless networks", *In Proceedings of the Conference on Applications, Technologies, Architectures, and Protocols for Computer Communication, ACM SIGCOMM Comput. Commun*, pp. 39-49, 1997.

[7] C. Ware, T. Wysocki and J. Chicharo, "Hidden terminal jamming problems in IEEE 802.11 mobile ad-hoc networks", *In Proceedings of the IEEE International Conference on Communications (ICC' 01)*, pp. 261-265, Helsinki, Finland, Jun. 2001.

[8] L. Kleinrock and F. Tobagi, "Packet switching in radio channels: Part I-Carrier sense multiple access modes and their throughput-delay characteristics", *IEEE Transactions on Communications*, 23(12), pp. 1400-1416, December 1975.

[9] A. Tanenbaum, *Computer networks*. Prentice-Hall, PTR, Upper Saddle River, NJ, 4th Edition, 2003.

[10] L. Kleinrock and F. Tobagi, "Random access techniques for data transmission over packet switched radio channels", *In Proceedings of National Computer Conference and Exposition (AFIPS' 75)*, pp. 187-201, May, 1975.

[11] Kwang-Cheng Chen and Ramjee Prasad, *Cognitive radio networks*. John Wiley, New York, 2009.

[12] J. Yeh, "Simulation of local computer networks: a case study", *Computer Networks*, vol. 3, pp. 401-417, 1979.

[13] A. Sugihara, K. Enomoto and I. Sasase, "Throughput performance of a slotted non-persistent CSMA with an adaptive array", *In Proceedings of the 6th IEEE International Symposium*, vol. 2, pp. 633-637, 1995.

[14] G. Bianchi, “Performance analysis of the IEEE 802.11 distributed coordination function”, *IEEE Journal on Selected Areas of Communications*, 18(3), pp. 535-547, 2000.

[15] F. A. Tobagi and L. Kleinrock, “Packet switching in radio channels: part II - The hidden terminal problem in carrier multiple-access and the busy-tone solution”, *IEEE Transactions on Communications*, 23(12), pp. 1417-1433, December 1975.

[16] P. Karn, “MACA: A new channel access method for packet radio”, *ARRL/CRRL Amateur Radio 9th Computer Networking Conference*, September 1990.

[17] V. Bharghavan, A. Demers, S. Shenker and L. Zhang, “MACAW: A media access protocol for wireless LAN’s”, *In Proceedings of the conference on Applications, Technologies, Architectures, and Protocols for Computer Communication (ACM SIGCOMM’ 94)*, pp. 212-225, London, UK, November 1994.

[18] C. L. Fullmer and J. J. Garcia-Luna-Aceves, “Floor acquisition multiple access (FAMA) for packet radio networks”, *In Proceedings of the conference on Applications, Technologies, Architectures, and Protocols for Computer Communication (ACM SIGCOMM’ 95)*, 25(4), pp. 262-273, Cambridge, MA, October 1995.

[19] IEEE Standard for Information Technology-Telecommunications and Information Exchange between Systems-Local and Metropolitan Area Networks-specific Requirements, “Part 11: Wireless LAN medium access protocol (MAC) and physical layer (PHY) specification”, *IEEE STD 802.11-2007 (Revision of IEEE Std 802.11-1999)*, C11184, June 2007.

[20] H. Zhai and Y. Fang, "Physical carrier sensing and spatial reuse in multi-rate and multi-hop wireless ad-hoc networks", *In Proceedings of the 26th Annual Joint Conference on the IEEE Computer and Communications Societies (INFOCOM' 06)*, 2006.

[21] G. Sharma, A. Ganesh and P. Key, "Performance analysis of contention based medium access control protocols", *IEEE Transactions on Information Theory*, 55(4), pp. 1665-1682, April 2009.

[22] Matthew S. Gast, *802.11 wireless networks: the definitive guide*. Second Edition, OReilly Media Inc., Sebastopol, California, 2005.

[23] X. Hong, M. Gerla, G. Pei and C. Chiang, "A group mobility model for ad-hoc wireless networks", *In Proceedings of the ACM International Workshop on Modeling and Simulation of Wireless and Mobile Systems (MSWiM' 99)*, August 1999.

[24] C. Bettstetter, "Smooth is better than sharp: a random mobility model for simulation of wireless networks", *In Proceedings of the 4th ACM International Workshop on Modeling Analysis and Simulation of Wireless and Mobile Systems (ACM MSWIM' 01)*, pp. 19-27, Rome, Italy, July 2001.

[25] T. Camp, J. Boleng and V. Davies, "A survey of mobility models for ad hoc networks research", *Wireless Communication and Mobile Computing (WCMC' 02): Special issue on Mobile Ad-Hoc Networking: Research, Trends and Applications*, 2(5), pp. 483-502, 2002.

[26] N. Sadagopan, F. Bai, B. Krishnamachari and A. Helmy, "PATHS: analysis of path duration statistics and their impact on reactive MANET routing protocols", *In Proceedings of the 4th ACM International Symposium on Mobile Ad-hoc Networking and Computing (ACM MobiHoc' 03)*, June 2003.

[27] P. Samar and S. B. Wicker, "On the behavior of communication links of node in a multi-hop mobile environment", *In Proceedings of the 5th ACM International Symposium on Mobile Ad-hoc Networking and Computing (ACM MobiHoc' 04)*, May 2004.

[28] J. Y. Le Boudec and M. Vojnovic, "Perfect simulation and stationarity of a class of mobility models", *In Proceedings of the 25th Annual Joint Conference on the IEEE Computer and Communications Societies (INFOCOM' 05)*, Miami, FL, March 2005.

[29] M. McGuire, "Stationary distribution of random walk mobility models for wireless ad-hoc networks", *In Proceedings of the 6th ACM International Symposium on Mobile Ad-hoc Networking and Computing (ACM MobiHoc' 05)*, pp. 90-98, May 2005.

[30] D. B. Johnson and D. A. Maltz, "Dynamic source routing in ad-hoc wireless networks", *Mobile Computing (Kluwer Academic)*, vol. 353, pp. 153-181, 1996.

[31] J. Yoon, M. Liu and B. Noble, "Random waypoint considered harmful", *In Proceedings of the 23rd Annual Joint Conference on the IEEE Computer and Communications Societies (IEEE INFOCOM' 03)*, vol. 2, pp. 1312-1321, July 2003.

[32] N. Sabah and A. Hocanin, “An improved random waypoint mobility model for wireless ad-hoc networks”, *International Conference on Information and Multimedia Technology (ICIMT’ 10)*, Hong Kong, China, November 2010.

[33] D. M. Blough, G. Resta and P. Santi, “A statistical analysis of the long-run node spatial distribution in mobile ad-hoc networks”, *ACM-Kluwer Wireless Networks*, 10(5), pp. 543-554 September 2004.

[34] C. Bettstetter, G. Resta and P. Santi, “The node distribution of the random waypoint mobility model for wireless ad-hoc networks”, *IEEE Transactions on Mobile Computing*, 2(3), pp. 257-269, September 2003.

[35] P. Nain, D. Towsley, B. Liu and Z. Liu, “Properties of random direction model”, *In Proceedings of the 25th Annual Joint Conference on the IEEE Computer and Communications Societies (INFOCOM’ 05)*, Miami, FL, March 2005.

[36] N. Bansal and Z. Liu, “Capacity, delay and mobility in wireless ad-hoc networks”, *In Proceedings of the 22nd Annual Joint Conference on the IEEE Computer and Communications Societies (INFOCOM’ 03)*, vol. 2, pp. 1553-1563, San Francisco, CA, March 2003.

[37] P. Gupta and P. R. Kumar, “The capacity of wireless networks”, *IEEE Transactions on Information Theory*, 46(2), pp. 388-404, March 2000.

[38] M. Grossglauser and D. Tse, “Mobility increases the capacity of ad-hoc wireless networks”, *In Proceedings of the 21nd Annual Joint Conference on the IEEE Computer and Communications Societies (INFOCOM’ 01)*, vol. 3, pp. 1360-1369, Alaska, USA, April 2001.

[39] Ai Hua Ho, Yao Hua Ho and Kien A. Hua, "Handling high mobility in next-generation wireless ad-hoc networks", *International Journal of Communication Systems*, 23(9-10), pp. 1078-1092, October 2010.

[40] Y. K. Hassan, M. H. A. El-Aziz and A. S. A. El-Radi, "Performance evaluation of mobility speed over MANET routing protocols", *International Journal of Network Security*, 11(3), pp. 128-138, November 2010.

[41] Geetha Jayakumar and Gopinath Ganapathi, "Reference point group mobility and random waypoint models in performance evaluation of MANET routing protocols", *EURASIP Journal on Computer Systems, Networks, and Communications*, December 2008.

[42] M. M. Qabajeh, A. H. Adballa, O. O. Khalifa and L. K. Qabajeh, "A cluster-based QoS multicast routing protocol for scalable MANETs", *Transactions on Internet and Information Systems*, 5(4), pp. 741-762, April 2011.

[43] A. Alshanyour and U. Baroudi, "A Simulation study: The impact of random and realistic mobility models on the performance of bypass-AODV in ad-hoc wireless networks", *EURASIP Journal on Wireless Communications and Networking*, 2010.

[44] D. D. Perkins, H. D. Hughes and C. B. Owen, "Factors affecting the performance of ad-hoc networks", *In Proceedings of the IEEE International Conference on Communications (ICC' 02)*, vol. 4, pp. 2048-2052, New York, USA, August 2002.

[45] Rituparna Ghosh and Stefano Basagni, "Mitigating the impact of node mobility on ad-hoc clustering", *In Proceedings of the Wireless Communications and Mobile Computing (WCMC' 08)*, 8(3), pp. 295-308, March 2008.

[46] N. Sabah and A. Hocanin, "Gamma random waypoint mobility model for wireless ad-hoc networks", *International Journal of Communication Systems, Wiley*, DOI: 10.1002/dac.2319, January 2012.

[47] J. Yoon, M. Liu and B. Noble, "A general framework to construct stationary mobility models for the simulation of mobile networks", *IEEE Transactions on Mobile Computing*, 5(7), pp. 860-871, May 2006.

[48] T. Camp, J. Boleng, B. Williams, L. Wilcox and W. Navidi, "Performance comparison of two location based routing protocols for ad-hoc networks", *In Proceedings of the 22nd Annual Joint Conference on the IEEE Computer and Communications Societies (INFOCOM' 02)*, vol. 3, pp. 1678-1687, November 2002.

[49] T. Chu and I. Nikolaidis, "On the artifacts of random waypoint simulations", *In Proceedings of the 1st International Workshop on Wired/Wireless Internet Communications (WWIC2002), in conjunctions with the International Conference on Internet Computing (IC '02)*, Las Vegas, USA, vol. 1, pp. 69-76, June 2002.

[50] C. Bettstetter, "Mobility modeling in wireless networks: categorization, smooth movement, and border effects", *ACM Mobile Computing and Communications Review*, 5(3), July 2001.

[51] E. M. Royer, P. M. Melliar-Smith and L. E. Moser, "An analysis of the optimum node density for ad-hoc mobile networks", *In Proceedings of the IEEE Interna-*

tional Conference on Communications (ICC' 01), Finland, vol. 3, pp. 857-861, August 2001.

[52] F. Bai, N. Sadagopan and A. Helmy, "Important: A framework to systematically analyze the impact of mobility on performance of routing protocols for ad-hoc networks", *In Proceedings of the 22nd Annual Joint Conference on the IEEE Computer and Communications Societies (INFOCOM' 03)*, vol. 2, pp. 825-835, San Francisco, CA, March 2003.

[53] C. Bettstetter and C. Wagner, "The Spatial node distribution of the random waypoint mobility model", *In Proceedings of the German Workshop Mobile Ad Hoc Networks (WMAN' 02)*, March 2002.

[54] C. Bettstetter, H. Hartenstein and X. Perez-Costa, "Stochastic properties of the random waypoint mobility model: Epoch length, direction distribution and cell change rate", *In Proceedings of the 5th ACM International Workshop on Modeling Analysis and Simulation of Wireless and Mobile Systems (ACM MSWIM' 02)*, Atlanta, USA, September 2002.

[55] E. Hyytia, P. Lassila and J. Virtamo, "Spatial node distribution of the random waypoint mobility model with applications", *IEEE Transactions on Mobile Computing*, 5(6), pp. 680-694, June 2006.

[56] W. Hsu, K. Merchant, H. Shu, C. Hsu and A. Helmy, "Weighted waypoint mobility model and its impact on ad-hoc networks", *SIGMOBILE Mobile Computing and Communications Review*, 9(1), pp. 59-63, January 2005.

[57] S. Lim, C. Yu and C. R. Das, "Clustered mobility model for scale-free wireless networks", *In Proceedings of the IEEE Local Computer Networks (IEEE LCN '06)*, FL, USA, pp. 231-238, November 2006.

[58] M. Gyarmati, U. Schilcher, G. Brandner, C. Bettstetter, Y. W. Chung and Y. H. Kim, "Impact of random mobility on the inhomogeneity of spatial distributions", *In Proceedings of the IEEE Global Telecommunications Conference (GLOBECOM' 08)*, LO, USA, pp. 1-5, December 2008.

[59] G. Resta and P. Santi, "An analysis of the node spatial distribution of the random waypoint model for ad-hoc networks", *In Proceedings of ACM Workshop on Principles of Mobile Computing (POMC' 02)*, pp. 44-50, Toulouse, France, October 2002.

[60] W. Navidi and T. Camp, "Stationary distributions for the random waypoint mobility model", *IEEE Transactions on Mobile Computing*, 3(1), pp. 99-108, August 2004.

[61] A. K. Mohammed, "Factors affecting the performance of ad-hoc networks", *In Proceedings of the 14th International Conference on Computer Communications and Networks (ICCCN' 05)*, pp. 49-54, October 2005.

[62] J. Yoon, M. Liu and B. Noble, "Sound mobility models", *In Proceedings of the 9th Annual International Conference on Mobile Computing and Networking (ACM Mobicom '03)*, pp. 205-216, San Diego, California, September 2003.

[63] R. M. de Moraes, F. P. de Araujo and A. S. L. Pontes, "A proposal to stabilize the random waypoint mobility model for ad-hoc network simulation", *In Proceedings*

of IEEE Wireless Communications and Networking Conference (WCNC' 10), pp. 1-6, Sydney, Australia, 2010.

[64] L. A. Santalo, *Integral geometry and geometric probability*. Addison-Wesley, 1976.

[65] A. Papoulis and S. U. Pillai, *Probability, random variables, and stochastic processes*. 4th Edition, McGraw-Hill, 2002.

[66] C. Yu, T. Shen, K. G. Shin, J. Y. Lee and Y. J. Suh, "Multi-hop transmission opportunity in wireless multi-hop networks", *In Proceedings of the 29th Annual Joint Conference on the IEEE Computer and Communications Societies (IEEE INFOCOM' 10)*, March 2010.

[67] S. H. Kim, D. W. Kim and Y. J. Suh, "A cooperative channel assignment protocol for multi-channel multi-rate wireless mesh networks", *Ad-Hoc Networks*, 9(5), pp. 893-910, 2011.

[68] K. Medepalli and F. A. Tobagi, "Throughput analysis of IEEE 802.11 wireless LANs using an average cycle time approach", *IEEE Global Communications Conference (GLOBECOM' 05)*, Saint Louis, USA, November 2005.

[69] K. Chen, S. H. Shah and K. Nahrstedt, "Dynamic bandwidth management in single-hop ad-hoc wireless networks", *Mobile Networks and Application*, pp. 199-217, 2005.

[70] A. Abdrabou and W. Zhuang, "Service time approximation in IEEEE 802.11 single-hop ad-hoc networks", *IEEE Transactions on Wireless Communications*, 7(1), pp. 305-313, January 2008.

[71] N. Gupta and P. R. Kumar, "A performance analysis of the 802.11 wireless LAN medium access control", *IEEE Journal on Communications in Information and Systems*, 3(4), pp. 279-304, September 2004.

[72] F. Cuomo, C. Martello, A. Baiocchi and F. Capriotti, "Radio resource sharing for ad-hoc networking with UWB", *IEEE Journal on Selected Areas in Communications*, 20(9), pp. 1722-1732, 2002.

[73] A. Hicham, Y. Souilmi and C. Bonnet, "Self-balanced receiver-oriented MAC for ultra-wide band mobile ad-hoc networks", *In Proceedings of IEEE Vehicular Technology Conference (VTC' 05)*, vol. 3, pp. 1514-1518, 2005.

[74] S. Kolenchery, J. Townsend and J. Freebersyser, "A novel impulse radio network for tactical military wireless communications", *In Proceedings of IEEE Military Communications Conference (MILCOM' 98)*, vol. 1, pp. 59-65, 1998.

[75] A. Muqattash and K. Marwan, "CDMA-based MAC protocol for wireless ad-hoc networks", *In Proceedings of the 4th ACM International Symposium on Mobile Ad-hoc Networking and Computing (ACM MobiHoc' 03)*, pp. 153-164, 2003.

[76] B. Radunovic and J. Y. Le Boudec, "Optimal power control, scheduling and routing in UWB networks", *IEEE Journal on Selected Areas in Communications*, 22(7), pp. 1252-1270, 2004.

[77] IEEE P802.11, "IEEE Standard for Wireless LAN Medium Access Control (MAC) and Physical Layer (PHY) Specifications", *IEEE Std P802.11 1997*, November 1997.

[78] M. Natkaniec and A. Pach, "An analysis of modified backoff mechanism in IEEE 802.11 Networks", *In Proceedings of the PolishGerman Teletraffic Symposium (PGTS 2000)*, Dresden, Germany, pp. 89-96, September 2000.

[79] H. Wu, K. Long, S. Cheng and J. Ma, "IEEE 802.11 DCF: Analysis and enhancement", *In Proceedings of the IEEE International Conference on Communications (ICC 2002)*, New York, USA, vol. 1, pp. 605-609, April 2002.

[80] N. Qiang, I. Aad, C. Barakat and T. Turletti, "Modeling and analysis of slow CW decrease in IEEE 802.11", *In Proceedings of the IEEE Conference Personal, Indoor Mobile Radio Communications (PIMRC 2003)*, Beijing, China, pp. 1717-1721, September 2003.

[81] Mohammad Hossein Manshaei, Gion Reto Cantieni, Chadi Barakat and Thierry Turletti, "Performance analysis of the IEEE 802.11 MAC and physical layer protocol", *In the IEEE International Symposium on a World of Wireless Mobile and Multimedia Networks (WOWMOM' 05)*, pp. 88-97, Taormina, Italy, June 2005.

[82] C. Foh and M. Zukerman, "Performance analysis of the IEEE 802.11 MAC protocol", *In Proceedings of the European Wireless 2002 Conference (EW' 02)*, pp. 184-190, Florence, Italy, February 2002.

[83] Y. Xiao and J. Rosdahl, "Performance analysis and enhancement for the current and future IEEE 802.11 MAC protocols", *ACM SIGMOBILE Mobile Computing*

and Communications Review (MC2R), special issue on Wireless Home Networks, 7(2), pp. 6-19, April 2003.

[84] F. Cali, M. Conti, and E. Gregori, "Dynamic tuning of the IEEE 802.11 protocol to achieve a theoretical throughput limit", *IEEE/ACM Transactions on Networking*, 8(6), pp. 785799, December 2000.

[85] H. Chhaya and S. Gupta, "Performance modeling of asynchronous data transfer methods of IEEE 802.11 MAC protocol", *Wireless Networks*, vol. 3, 217-234, 1997.

[86] Y. Wang and J. J. Garcia-Luna-Aceves, "Performance of collision avoidance protocols in single-channel ad-hoc networks", *In Proceedings of the 10th IEEE International Conference on Network Protocols (ICNP' 02)*, pp. 68-77, Paris, France, November 2002.

[87] M. Carvalho and J. Aceves, "Scalable model for channel access protocols in multihop ad-hoc networks", *In Proceedings of the 9th Annual International Conference on Mobile Computing and Networking (ACM Mobicom '04)*, Pennsylvania, USA,September 2004.

[88] Kaixin Xu, Mario Gerla and Sang Bae, "Optimization of IEEE 802.11 parameters for wide area coverage", *IEEE Global Communications Conference (GLOBECOM' 02)*, Taipei, China, November 2002.

[89] K. Xu, M. Gerla and S. Bae, "How effective is the IEEE 802.11 RTS/CTS handshake in ad-hoc networks", *IEEE Global Communications Conference (GLOBECOM' 02)*, Taipei, China, November 2002.

[90] D. Valerio, L. De Cicco, S. Mascolo, F. Vacirca and T. Ziegler, “Optimization of IEEE 802.11 parameters for wide area coverage”, *IEEE Global Communications Conference (GLOBECOM)*, Taipei, China, Nov. 2002.

[91] D. Valerio, L. De Cicco, S. Mascolo, F. Vacirca and T. Ziegler, “How effective is the IEEE 802.11 RTS/CTS handshake in ad-hoc networks?”, *In Proceedings of MEDHOCNET’ 06*, June 2006

[92] Daniel H. Greene and Donald E. Knuth, *Mathematics for the Analysis of Algorithms*, Birkhäuser Boston. 3rd edition, 1990.

[93] M. Grossglauser and D. Tse, “Mobility increases the capacity of ad-hoc wireless networks”, *IEEE/ACM Transactions on Networking*, 10(4), pp. 477-486, August 2002.

[94] F. Dai and J. Wu, “Distributed dominant pruning in ad hoc wireless networks”, *In Proceedings of the IEEE International Conference on Communications (ICC)*, Alaska, USA, May 2003

[95] N. Li, J. Hou and L. Sha, “Design and analysis of an MST-based topology control algorithm”, *In Proceedings of the 22nd Annual Joint Conference on the IEEE Computer and Communications Societies (INFOCOM’ 03)*, pp. 1702-1712, San Francisco, CA, March 2003.

[96] Charles E. Perkins, Elizabeth M. Royer and Samir R. Das, “IP flooding in ad-hoc networks”, *Internet draft (draft-ietf-manet-bcast-00.txt)*, 2001.

[97] N. Sabah and A. Hocanin, “The performance of IEEE 802.11 RTS/CTS with random waypoint mobility”, *In Proceedings of the 6th International Symposium on Electrical and Electronics Engineering and Computer Systems (EEECS ’10)*, TRNC, Turkey, November 2010.

[98] Ravi Jain, Dan Lelescu and Mahadevan Balakrishnan, “Model T: An empirical model for user registration patterns in a campus wireless LAN”, *In Proceedings of the 11th Annual International Conference on Mobile Computing and Networking (ACM Mobicom ’05)*, pp. 170-184, Cologne, Germany, August 2005.

[99] M. Kyriakakos, N. Frangiadakis, L. Merakos and S Hadjiefthymiades, “Enhanced path prediction for network resource management in wireless LANs”, *IEEE Wireless Communications*, 10(6), pp. 62-69, December 2003.

[100] Youssef Iraqi, Majid Ghaderi and Raouf Boutaba, “Enabling real-time all-IP wireless networks”, *In Proceedings of IEEE Wireless Communications and Networking Conference (WCNC ’04)*, vol. 3, pp. 1500-1505, March 2004.

[101] V. Gupta and A. Dixit, “The design and deployment of a mobility supporting network”, *In Proceedings of International Symposium on Parallel Architectures, Algorithms, and Networks (I-SPAN ’96)*, pp. 228-234, Beijing, China, June 1996.

[102] M. X. Cheng, M. Cardei, Jinhua Sun, Xiaochun Cheng, Lusheng Wang, Yingfeng Xu and Ding-Zhu Du, “Topology control of ad-hoc wireless networks for energy efficiency”, *IEEE Transactions on Computers*, 53(12), 1629-1635, December 2004.

[103] V. S. Borkar and D Manjunath, "Distributed topology control of wireless networks", *In Proceedings of the 3rd International Symposium on Modeling and Optimization in Mobile, Ad-Hoc, and Wireless Networks (WIOPT '03)*, pp. 155-163, Trentino, Italy, April 2005.

[104] C. Bettstetter, "On the connectivity of ad-hoc networks", *Computer Journal, Special Issue on Mobile and Pervasive Computing*, 47(4), pp. 432-447, July 2004.

[105] Wing Ho Yuen and Chi Wan Sung, "On energy efficiency and network connectivity of mobile ad-hoc networks", *In Proceedings of the 23rd International Conference on Distributed Computing Systems (ICDCS '03)*, pp. 38-45, Providence, Rhode Island, USA, May 2003.

[106] M. Zonoozi and P. Dassanayake, "User mobility modeling and characterization of mobility patterns", *IEEE Journal on Selected Areas in Communications*, 15(7), pp. 1239-1252. September 1997.

[107] N. Sabah and A. Hocanin, "The effect of finite-population on the performance of IEEE 802.11 ad-hoc networks", *In Proceedings of the 6th International Symposium on Electrical and Electronics Engineering and Computer Systems (EEECS '10)*, TRNC, Turkey, November 2010.

[108] L. Kleinrock, *Queueing systems theory*. vol. I, Wiley, New York, 1975.

[109] J. Jackson, "Job shop-like queueing systems", *Manage. Sci.*, 10 (1), pp. 131-142, 1963.

[110] W. Gordon and G. Newell, "Closed queueing systems with exponential servers", *Operation Research*, 15(2), pp. 254-265, 1965.

[111] R. Rindzevicius, D. Pokaitis and B. Dekeris, "Performance measures analysis of M/M/m/K/N systems with finite customer population", *Elektronika ir Elektrotechnika- Kaunas: Technologija*, 3(67), pp. 65-70, 2006.

[112] G. Zeng, H. Zhu and I. Chlamtac, "A novel queueing model for 802.11 wireless LANs", *In Proceedings of WNCG Wireless Networking Symposium*, Austin, Texas, October 2003.

[113] M. Ozdemir and A. B. McDonald, "An M/MMGI/1/K queuing model for IEEE 802.11 ad-hoc networks", *In Proceedings of the First ACM International Workshop on Performance Evaluation of Wireless Ad Hoc, Sensor, and Ubiquitous Networks, ACM Press*, pp. 107111, 2003.

[114] O. Tickoo and B. Sikdar, "Queueing analysis and delay mitigation in IEEE 802.11 random access MAC based wireless network", *In Proceedings of the 24th Annual Joint Conference on the IEEE Computer and Communications Societies (INFOCOM' 04)*, Hong Kong, China, March 2004.

[115] S. M. R. Iravani and V. Krishnamurthy, "Workforce agility in repair and maintenance environment", *Manufacturing & Service Operations Management 9(2)*, pp. 168-184, 2007.

[116] D. Gross and C. M. Harris, *"Fundamentals of queueing theory"*, New York, Wiley, 1985.

[117] B. D. Bunday and R. E. Scraton, "The GIM/r machine interference model", *European Journal of Operational Research 4*, pp.399-402, 1980.

[118] L. Kleinrock, *Queuing systems: problems and solutions*. Wiley, New York, 1996.

[119] J. Little, "A proof of the queuing formula L = λ W", *Operations Research*, 9(3), pp. 383-387, 1961.

[120] S. M. R. Iravani and B. Kolfal, "When does the $c\mu$ rule apply to finite population queueing systems", *Operations Research Letters 33*, pp. 301-304, 2005.

[121] J. Bellamy, *Digital telephony*. Wiley, New York. 1982.

APPENDIX .

The expected value of Y is given as follows

$$
\begin{aligned}
E[Y] &= \int_0^\tau y\, f_Y(y)\, dy, \\
&= \int_0^\tau y\lambda\, e^{\lambda(y-\tau)}\, dy, \\
&\text{let } u = \lambda(y-\tau),\ \ du = \lambda dy \\
&= \int_0^\tau \frac{u+\lambda\tau}{\lambda}\, e^u\, du, \\
&= \frac{1}{\lambda}\int_0^\tau u\, e^u\, du + \tau\int_0^\tau e^u\, du, \\
&= \frac{u}{\lambda}\, e^u - \frac{1}{\lambda}\int_0^\tau e^u\, du + \tau\int_0^\tau e^u\, du, \\
&= \frac{u}{\lambda}\, e^u - \frac{1}{\lambda}\, e^u + \tau e^u \Big|_0^\tau, \\
&= \frac{u-1+\lambda\tau}{\lambda}\, e^u \Big|_0^\tau, \\
&\text{Substitute for } u = \lambda(y-\tau) \\
&= \frac{\lambda y - 1}{\lambda}\, e^{\lambda(y-\tau)} \Big|_0^\tau, \\
&= \tau - \frac{1-e^{-\lambda\tau}}{\lambda}. \qquad (1)
\end{aligned}
$$

The expected steady state speed for a given node can be obtained as follows:

$$\begin{aligned}
E[V_{ss}] &= \lim_{T\to\infty} \frac{1}{T}\int_0^T v(t)\,dt, \\
&= \lim_{T\to\infty} \frac{\sum_{j=1}^{K(T)} v_j\, t_j}{T}, \\
&= \lim_{T\to\infty} \frac{\sum_{j=1}^{K(T)} d_j}{\sum_{j=1}^{K(T)} t_j + (t_p)_j}, \\
&= \lim_{T\to\infty} \frac{\frac{1}{K(T)}\sum_{j=1}^{K(T)} d_j}{\frac{1}{K(T)}\sum_{j=1}^{K(T)} t_j + (t_p)_j}, \\
&= \frac{E[d]}{E[t] + E[t_p]}. \qquad (2)
\end{aligned}$$

$$\int x^n e^{ax}\,dx = e^{ax}\sum_{k=0}^{n} \frac{(-1)^k\, n!}{(n-k)!\, a^{k+1}}\, x^{n-k}. \qquad (3)$$

Using (3). The pdf of the steady state speed without pausing can be simplified as

follows:

$$
\begin{aligned}
f_{V_{ss}}(v) &= \frac{v^{\alpha-2}\, e^{-v/\beta}}{\int_{V_{min}}^{V_{max}} v^{\alpha-2}\, e^{-v/\beta}\, dv}, \\
&= \frac{v^{\alpha-2}\, e^{-v/\beta}}{e^{-v/\beta} \sum_{k=0}^{\alpha-2} \frac{(-1)^k\, (\alpha-2)!\, v^{\alpha-k-2}}{(\alpha-k-2)!\, (-1/\beta)^{k+1}}} \Bigg|_{V_{min}}^{V_{max}}, \\
&= \frac{v^{\alpha-2}}{-(\alpha-2)! \sum_{k=0}^{\alpha-2} \frac{v^{\alpha-k-2}}{(\alpha-k-2)!\, (1/\beta)^{k+1}}} \Bigg|_{V_{min}}^{V_{max}}, \\
&\text{let} \quad n = \alpha - k - 2 \\
&= \frac{v^{\alpha-2}}{(\alpha-2)! \sum_{n=0}^{\alpha-2} \frac{v^n}{n!\, (1/\beta)^{-n+\alpha-1}}} \Bigg|_{V_{max}}^{V_{min}}, \\
&= \frac{v^{\alpha-2}}{\beta^{\alpha-1}\, (\alpha-2)! \sum_{n=0}^{\alpha-2} \frac{(v/\beta)^n}{n!}} \Bigg|_{V_{max}}^{V_{min}}. \qquad (4)
\end{aligned}
$$

Using (3). The expected traveling time with pausing can be simplified as follows:

$$
\begin{aligned}
E[t] &= \frac{E[d]}{\beta^\alpha\, \Gamma(\alpha)} \int_{V_{min}}^{V_{max}} v^{\alpha-2}\, e^{-v/\beta}\, dv, \\
&= \frac{E[d]}{\beta^\alpha\, \Gamma(\alpha)}\, e^{-v/\beta} \sum_{k=0}^{\alpha-2} \frac{(-1)^k\, (\alpha-2)!\, v^{\alpha-k-2}}{(\alpha-k-2)!\, (-1/\beta)^{k+1}} \Bigg|_{V_{min}}^{V_{max}}, \\
&= \frac{-E[d]}{\beta^\alpha\, (\alpha-1)}\, e^{-v/\beta} \sum_{k=0}^{\alpha-2} \frac{v^{\alpha-k-2}}{(\alpha-k-2)!\, (1/\beta)^{k+1}} \Bigg|_{V_{min}}^{V_{max}}, \\
&\text{let} \quad n = \alpha - k - 2 \\
&= \frac{E[d]}{\beta^\alpha\, (\alpha-1)}\, e^{-v/\beta} \sum_{n=0}^{\alpha-2} \frac{v^n}{n!\, (1/\beta)^{-n+\alpha-1}} \Bigg|_{V_{max}}^{V_{min}}, \\
&= \frac{E[d]\, \beta^{\alpha-1}}{\beta^\alpha\, (\alpha-1)}\, e^{-v/\beta} \sum_{n=0}^{\alpha-2} \frac{(v/\beta)^n}{n!} \Bigg|_{V_{max}}^{V_{min}}, \\
&= \frac{E[d]}{\beta(\alpha-1)}\, e^{-v/\beta} \sum_{n=0}^{\alpha-2} \frac{(v/\beta)^n}{n!} \Bigg|_{V_{max}}^{V_{min}}. \qquad (5)
\end{aligned}
$$

APPENDIX